

UNIVERSITATEA “LUCIAN BLAGA” din SIBIU
FACULTATEA DE INGINERIE

TEZA DE DOCTORAT
(SUMMARY OF Ph.D. THESIS)

*Research Paper Regarding the Improvement of
Laser Cutting Technological Equipment with
Numerical Control used in automotive*

Ing. Mircea Sorin TÎRNOVEAN

Scientific coordinator
Prof.univ.dr.ing Octavian BOLOGA

SIBIU 2016

Summary

Chapter 1

Elements of Automated System Theory

<i>1.1 Introductory Notions. The Purpose of the Automated Command and Control Techniques.....</i>	<i>1</i>
<i>1.2 General terms of automated systems. Definition and structure</i>	<i>1</i>
<i>1.2.1. The controller functions in automatic control systems</i>	<i>3</i>
<i>1.2.2. The main problems of automatic systems</i>	<i>4</i>
<i>1.2.3. Aspects relating analysis and synthesis of automatic systems</i>	<i>4</i>
<i>1.3. Representing in the form of block scheme</i>	<i>5</i>
<i>1.4. Transfer Function</i>	<i>5</i>
<i>1.5. The algebra of functional schemes, with the functions of transfer.....</i>	<i>9</i>
<i>1.6. Performance automatic continuous linear systems. Of performance Indices. 10</i>	
<i>1.7. Stability of linear systems continue</i>	<i>13</i>

Chapter 2

Present Status of Laser Cutting Machine Processes with Numerical Control

<i>2.1 Main Types of Operations to be Undertaken within the Machine Processing Industry</i>	<i>19</i>
<i>2.2. Laser Cutting</i>	<i>20</i>
<i>2.3 The Structural Analysis of Laser Cutting Machines with Numerical Control</i>	<i>25</i>
<i>2.4. Kinematic chains, for advance of laser cutting machines</i>	<i>27</i>
<i>2.4.1 General, structure.....</i>	<i>27</i>
<i>2.4.2. Motion control.....</i>	<i>29</i>
<i>2.5. The tracking error, the position error, the contouring error</i>	<i>31</i>
<i>2.6. Control strategies</i>	<i>34</i>
<i>2.6.1. PID Controller</i>	<i>34</i>
<i>2.6.2. Feed-forward Controller</i>	<i>37</i>

2.6.3. Cross-coupling Controller	40
2.6.4. Overview of control strategies	42
2.7. Preliminary conclusions and research objectives	44

Chapter 3

Mathematical Model of the Feeder Linkages taken from the Laser Cutting Machine Structure with Numerical Control

3.1. Flow Chart of the System	51
3.2. Defining the Transfer Functions of the System	52
3.3. Position Controller	56
3.4. The Model for Forces and Moments of Resistance	58
3.5. Conclusions	63

Chapter 4

The Simulation Study of Feeder Linkages' Behaviour Comprised by a Laser Cutting Machine with a Numerical Control Structure, During Different Operational Modes

4.1. Initial Data	65
4.2 Elements of the kinematic of the movement uniaxial	66
4.3 The calculus of forces and moments of resistance for the X axis (displacement linkages for table movement).....	69
4.4 Calculation of forces and moments resistant Y axis(kinematic chain, of displacement horizontally to the cutting head).....	73
4.5 The Simulation Study of the Uniaxial Fast Positioning Mode	76
4.6 Simulation Study of the Biaxial Outlining	85
4.6.1. Interpolation Algorithm for the Techniques Using Reference Words	87
4.6.2 Radius error, and chord error	91
4.6.3 The calculation of the sampling period	93
4.6.4 The chart simulation	94
4.6.5 Simulations	96
4.6.6. Errors due the algorithm, of interpolation	103
4.7 The Simulation Study for Generating the 90° Corners	103

Chapter 5

Applied Experimental Research in Relation to the Laser Cutting Machines with Numerical Control

<i>5.1. Equipment Used</i>	109
<i>5.2. Processed Parts</i>	112
<i>5.3. Material used</i>	115
<i>5.4 Experimental Research on the Outline Cutting Precision</i>	116
<i>5.5 Experimental Research on the Cutting Precision for the 90° Corners</i>	128
<i>5.6. Applied Research Regarding the Carving Process of Semi-Finished Products</i> .	131
<i>5.6.1. The cutting</i>	131
<i>5.6.2. Problems arising in using cutting plans</i>	134
<i>5.6.3. Method of calculating the utilization of the material, based on image processing</i>	135

Chapter 6

Final Conclusions and Contributions

<i>6.1. Final Conclusions</i>	141
<i>6.2 Personal Contributions</i>	144
<i>6.3. Possible directions taken by the present research paper</i>	145

<i>Annexis</i>	146
----------------------	-----

<i>Bibliography</i>	155
---------------------------	-----

Keywords:

CNC laser cutting machine, CAM techniques, block scheme, laser cutting, kinematic chains, motion control, flow chart, transfer functions, position controller, tracking error, control strategies, forces and moments resistant, simulation, interpolation algorithm, cutting precision, radius error, chord error, feed drives, laser profiling, cutting plans

Chapter 1

Elements of Automated System Theory

1.1. Introductory Notions. The Purpose of the Automated Command and Control Techniques

The industrial automation processes are characterised by the presence of machinery and apparatus that have an automated functionality and which make up, most of the time, very complex installations. These automatization processes or modern automatization methods are based largely on automated command and control techniques.

A particular feature of the automated command and control system constitutes the fact that during their operation, a specific adjustment takes place for certain measurements (signals), accompanied by information processing operations. As automated command and control techniques are widely independent from the apparatus with which the process is undertaken, these fields of application must be subordinated to the science of systems; and that is the reason why, what follows represents the basic considerations of the theory of automated systems.

Chapter 2

Present Status of Laser Cutting Machine Processes with Numerical Control

2.1. Main Types of Operations to be Undertaken within the Machine Processing Industry

The processing operations depend greatly on the shape of the processed part and on the form and type of the semi-finished product. As such, for extensive unregularly shaped parts that are obtained from prismatic, cylinder or by casting semi-finished products, the procedure used is that of milling. For revolution parts obtained from cylinder semi-finished products, the procedure used is that of turning; and for plane parts obtained from thin metal sheet plate, a group of procedures generically named profiling is used.

The semi-finished products of the thin metal sheet plate present a much lower thickness compared to the other two sizes (length and width) and their processing is usually made within the plane of the two main sizes, length (X) and width (Y), more exactly the XOY plane. The technological displacements on the Z-axis usually represent positioning movements undertaken outside the processing operations.

The profiling operational group comprises:

- Oxiacetic flame cutting (oxy-gaz/oxy- fuel)
- Plasma beam cutting
- Laser cutting
- Waterjet cutting
- Electro-erosion with thread-shaped electrode
- Punching operations with the use of numerical control punching machines

2.2. Laser Cutting

The LASER acronym stands for Light Amplification by Stimulated Emission of Radiation and the first applications have been reported as early as the 50's, during the XXth century.

The cutting technology for plane parts using a laser beam has already been in use for a relative long period of time, which practically coincides with the advent of lasers, but the large scale massive introduction of technological equipment with numerical control has led to the industrial spread of the process, especially in the last three decades of the last century. During the last years, an accelerated development of the three-dimensional (3D) cutting equipment is noted, that expands the technological possibilities of the procedure.

The laser cutting procedure (fig.2.2) is done by melting/ evaporating the material using a focused laser beam as heat source. Coaxially, alongside the laser beam is introduced an auxiliary gas to built the energetic jet [95, 99, 104].

In figure 2.3, is presented the dependency between the laser beam power, the type and thickness of the material and in figure 2.4. is presented the dependency between the cutting feed rate and the thickness of the material for a laser with 2600W, using CO₂ as an auxiliary gas. In figure 2.5. is presented the dependency between the thickness of the semi-finished product and its' roughness when cutting unalloyed steel [154].

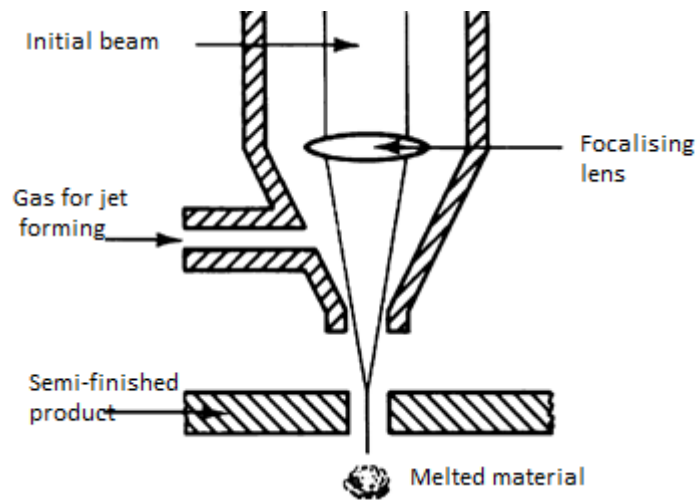


Fig. 2.2: Laser cutting procedure [95]

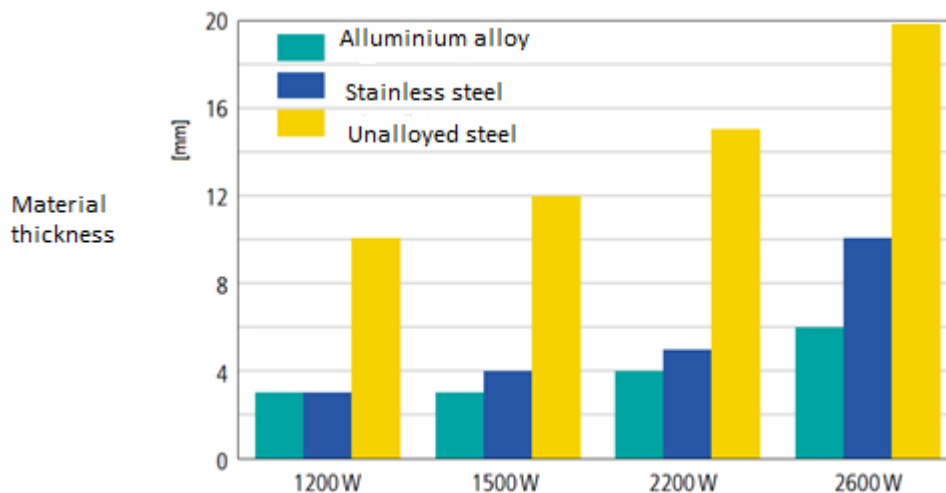


Fig. 2.3: The dependency between the laser beam power and the type and thickness of the material [154]

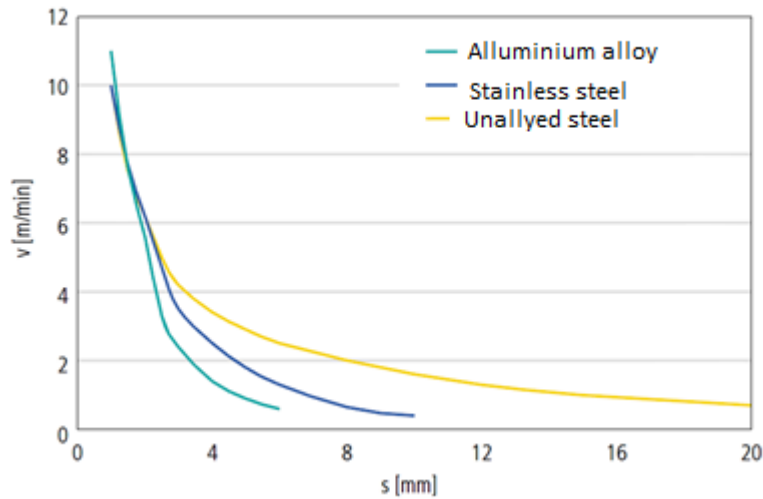


Fig. 2.4: The dependency between the cutting feed rate and the thickness of the material for a laser with 2600W, using CO_2 as an auxiliary gas [154]

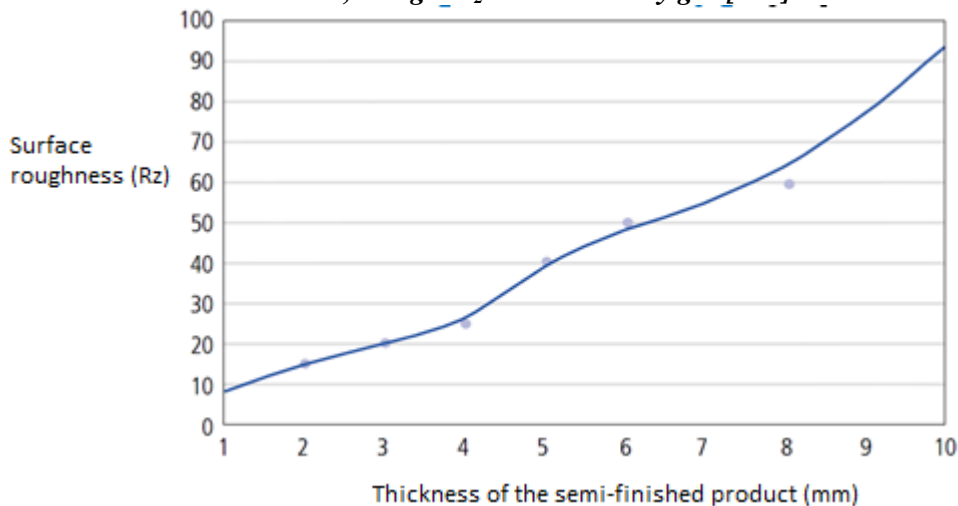


Fig. 2.5: The dependency between the thickness of the semi-finished product and its' roughness when cutting unalloyed steel [154]

Laser processing is characterised by a 10...20 increase in productivity, compared to the oxiacetylenic cutting procedure or that of mechanical cutting. Furthermore, there are certain advantages of laser cutting [22, 27, 46, 48, 59, 76, 81, 84, 103, 104]:

- high speed technological rates during the cutting operation of the semi-finished product;
- reduced technological losses due to low values of the laser beam diameter (with values between 0.2...0.5mm);
- the precision of the processed parts is superior to those obtained by similar means (oxy-fuel and plasma cutting);
- reduced thermal influenced area and thus a better roughness of the processed surfaces;
- the possibility of processing certain parts with complex shapes;
- wide range of processed materials.

Amongst the disadvantages [55, 81, 86, 90, 99, 103, 104, 148] of using a laser cutting system to be mentioned:

- the numerical control machine-tool equipments with laser cutting functionality have relatively high-cost purchasing prices (compared to the other profiling machinery or even to the splinting processing machines);
- there is a limit to the thickness of the materials to be cut (limit between 10-15mm);
- certain materials (Al alloys and Cu alloys) can reflect the laser beam, fact that could influence the performances registered by the cutting procedure in a negative way.

2.3. The Structural Analysis of Laser Cutting Machines with Numerical Control

Present day laser cutting machines are, in their majority, produced with numerical control units that ensures the control of relative displacements between the metal sheet and the work units that sustain the laser beam. Moreover, the CNC (Computer Numerical Control) assures and maintains the technological parameters of the process within the established limits.

The structural layout of a laser cutting machine with numerical control is shown in figure 2.7.

The machine presented in figure 2.7. is used for plane cutting of semi-finished products of the metal sheet type. As such, the mobile elements of the machine execute movements controlled by the numerical control equipment on 3 translation axes, X, Y and Z. This type of machinery is the most widely used equipment and the most representative for laser cutting processes.

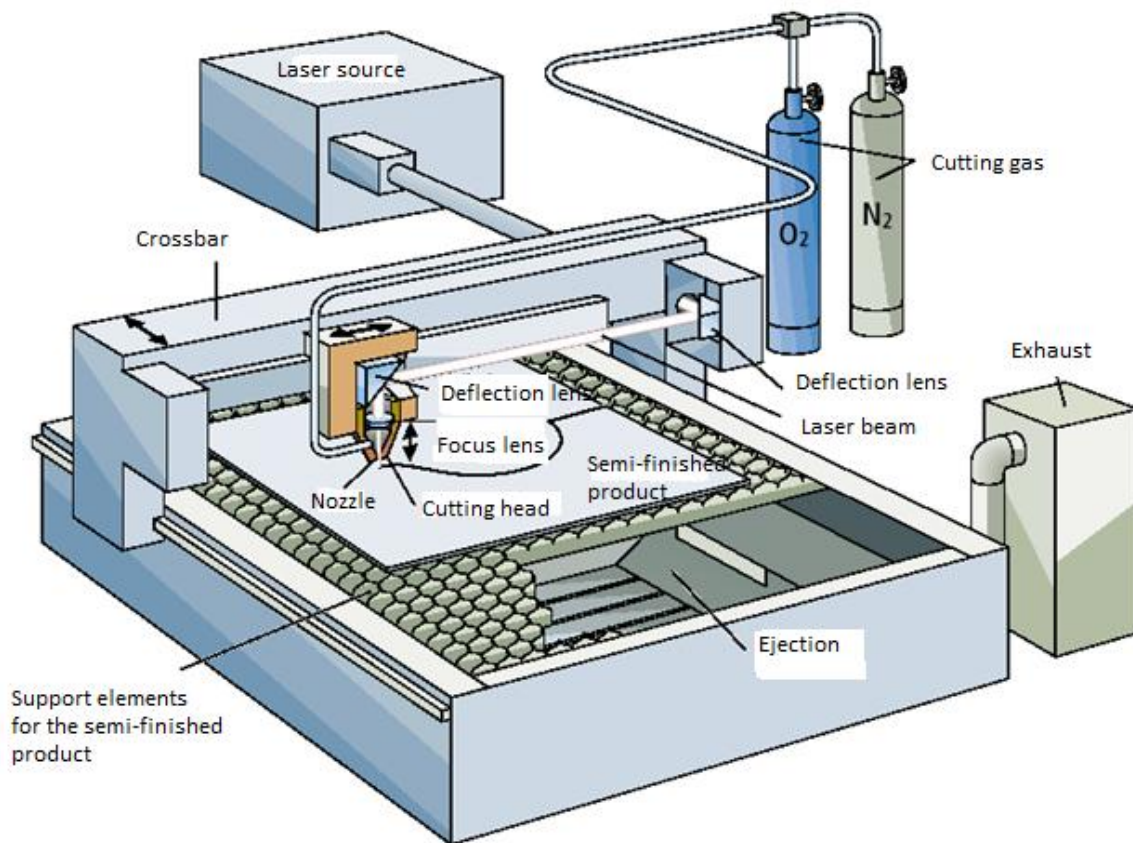


Fig. 2.7: The structural layout of a laser cutting machine with numerical control and 3 axes (X, Y, Z) [115]

2.6. Preliminary Conclusions and the Objective of the Present Research

Based on the information presented in this chapter, certain conclusions can be formed and presented in what follows.

The laser cutting technology of the semi-finished products - metal-sheet type- has been for a long time, a fully-developed technology used on industrial scale.

The structure of the laser cutting machines with numerical control is relatively standardized, mainly divided into two types: plane cutting machines with three numerical control

axes and spatial cutting machine with five numerical controlled axes. The research conducted according to the present paper makes reference to the plane cutting machines, due to their higher level of usage.

At the linkage level of these machines there are two major types of transmissions: ball screw mechanisms for the X and Y axes and belt mechanisms for the Z-axis.

The actuation of the linkages is made using control systems for closed loops adherent to position adjustment movements (here including the speed adjustment inner loop) or per short servo-systems/ mechanisms.

The most encountered execution element, or the movement source, is represented by the electric servo motor with direct current. But there are other applications that use a synchronous servo motor with alternative current or a stepping motor.

The usage of the synchronous servo motor, which remains the most used solution at present day, is not entirely justified, in the conditions in which the technological forces of resistance are relative low in comparison to the processing procedures.

Furthermore, the usage of a stepping motor, although reduces the manufacturing costs of the machine, does not ensure the best dynamic performances or precision, as obtained by means of the other two types of motors.

In conclusion, the best price-performance ratio is assured by the usage of the direct current servo motor, which as mentioned above, is the most widely used application. As such, the undertaken research has taken into consideration this particular version.

Thus it can be concluded that at the structural level, level of transmission and actuation, the laser cutting machines with numerical control are similar to the other types of numerical control equipment, especially with the splinting machines (turner milling machines). This similarity goes as far as feeder linkages are involved, where practically there are no differences between the laser cutting machines, milling machines and turners.

Taking into consideration the costs adherent to the working unit, costs that include the laser cutting head, the price for such an equipment with numerical control is higher than that of splinting cutting machines with numerical control.

Thereby a contradictory situation arises with the case of the laser cutting machine: structure, transmission and actuation are practically identical, processing precision at a significantly lower value than of those for the splinting processing procedure. Until present day, the laser cutting machines used to compensate for this disadvantage by means of higher productivity, as compared to the splinting processing, but which in time led to a quick compensation of the high price for the machinery. Recent developments of the equipment and for plasma, waterjet cutting machinery has led to an increased precision of processed parts by means of current methods and under the conditions according to which the productivity level is practically the same with that of the laser cutting machines; while the structure, transmission and actuation are far more simple and thus the costs adherent to them are reduced.

As such the niche technology taken up by the laser cutting machinery is narrowed even further, the precision level is lower than that of splintering processes and more and more closer to that of plasma and waterjet processing; making the initial costs for the machine even greater than compared to the splinting and plasma, waterjet cutting procedures.

One of the solutions to this problem, which will be investigated in the present paper, represents the increase in precision for processed parts using the laser cutting procedures with numerical control, by adjusting the parameters for the control systems of the feeder linkages. The improved structure allows the adjustment of these parameters with the purpose of enhancing processing precision.

The literature in the field approaches this idea with an increased level of novelty especially by implementing high-performance adjustment algorithms. The only problem is that these solutions must be applied during the design stage of the machine, and are not efficient in cases in which the increase is desired for an already existing equipment.

The modern laser cutting machinery with numerical control allows the interference with adjustment parameters for the control system of the movement, from the operator panel. These parameters are accessible from the menu of set values of the CNC equipment. There are also numerous practical problems to this approach:

- the vast majority of users do not know the significance of these parameters which, in most cases, are not explained in operating manuals. The lack of such explanations is due to the fact that the manufacturers of such machinery are mostly integrators, assembling the modules received from various producers. As such the laser cutting machine is manufactured by one company and the numerical control equipment by another and thus the omissions from the operating manuals;
- generally speaking, the opinion that these parameters have factory pre-settings and their adjustment is not necessary, is widely spread. This fact is only partially true, because the factory adjustments cannot take into consideration all the specific conditions that might occur at the performance location of the machinery. Furthermore, these conditions can change in time, making necessary a new adjustment.
- there is this "fear" of the user to intervene with these parameters because their wrong/erroneous adjustment can highly affect the processing precision. This thing is true but, also, as it is shown in the present paper, a corresponding adjustment can lead to a significant improvement of precision.

Interventions made at the level of adjustment parameters, regardless if made during the design phases or that of operation, must be based on the theoretical fundamental notions correspondent to the functionality of the feeder system. According to the literature in the field, the establishment of certain mathematical models for the feeder linkages can facilitate this method. There are also certain problematic aspects that can be summarised as follows:

- the proposed models display a high complexity level which make them difficult to be understood by the machine user;
- a series of phenomena are taken into consideration, such as, technological forces or frictions that have a significant influence during splinting processes and that are practically insignificant in case of metal sheet laser cutting operations.

Another problem to be taken into consideration, concerns a national specificity for metal sheet cutting using laser cutting machines with numerical control. More exactly, it is referred to the exceptionally high costs inhered for the specific CAD/CAM software packages, especially those that offer the possibility of carrying out automatic carving patterns. The fact that the vast majority of Romanian companies do not use such programmes, creates a series of specific problems. For some of these problems, the present research paper attempts to give applied solutions to help improve the functionality of the equipment.

As a summary, it can be stated that the main objectives of the paper are as follows:

From the theoretical reseach point of view

- *The establishment of a mathematical model for the feeder linkages that allows the highlight of the main adjustment parameters adherent to the movement control systems, taken from the feeder linkages of the laser cutting machine with numerical control.* The purpose is to make the parameters of the model coincide, to a greater extend, with the adjustment parameters accesable from the command panel of the numerical control equipment. Furthermore, it is intended that the mathematical model, to be kept as simple as possible and as closer to the understanding level of the machine operator and without affecting its' efficiency.
- *The performance of simulation diagrams that allow, based on the mathematical model aforementioned, the study of the feeder linkages' behaviour in various functioning conditions.* As such, the user can evaluate the effect produced by the adjustment of parameters through simulation, with all the advantages adherent to this fact. The focus lyes with fast displacements, outlining operations and the generation of 90° corners.

- *The performance of a simulation study, that highlights the influence of the adjustment parameters over the performance of the feeder linkages and implicitly over the processing precision of the laser cutting machinery with numerical control.* The study will allow the drafting of certain recommendations and strategies to be followed for each functioning mode of the machine. It will be permanently taken into consideration that the mathematical model mentioned above, as well as the simulation study, to be accessible in terms of complexity and software, hardware and financial resources, to the average user and to be applied within a workshop that utilises laser cutting machines with numerical control.

From the experimental research point of view

- *Experimental validation of the theoretical solutions needed for improving the precision level of processed parts by means of a laser cutting machine with numerical control.* This implies the processing of certain parts, with different values of the adjustment parameters adherent to the motion control systems, followed by dimensional measurements that allow the precise evaluation of the processed parts. The adjustment parameters, set based on the simulation studies will be monitored to see if they lead to the improvement of the level of precision. The experimental results will be highlighted as representing the changes proposed for the outlining and generation of 90° corner working mode.
- *The development of a method that allows the calculus of the materials' degree of usage from a carving pattern, based on image processing operations.* This method will allow, even those companies that do not have performant CAD/CAM software packages, to estimate the efficiency with which the metal sheet semi-finished product is used and to make the necessary measurements; production cost estimates and drafting a price offer for the clients, or to adjust the carving patterns with the purpose of increasing the level of usage for the material.

Chapter 3

Mathematical Model of the Feeder Linkages taken from the Laser Cutting Machine Structure with Numerical Control

3.1. Flow Chart of the System

The flow chart of a feeder linkage, from a laser cutting machine-tool equipment with CNC, is shown in figure 3.1.

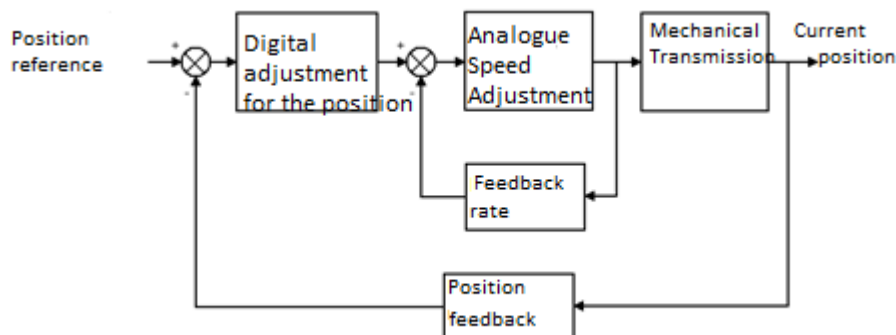


Fig. 3.1: The flow chart of a feeder linkage from a laser cutting machine-tool equipment with CNC

There are two adjustment loops; an external one for position, that in most cases is of numerical/digital nature and an internal one for speed, that is usually of analog type.

The closing of a speed loop is done by means of a position feedback transducer. The laser cutting machine-tools with CNC are usually equipped with a photoelectric rotary incremental numerical transducer. The feedback rate and respectively the closing of the speed feedback loop is done with the help of a speed transducer, which in case of a direct current servo motor representing the operational element, is represented by a tachogenerator.

The CNC equipment generates the kinematic reference values (position, speed, acceleration), by processing the information found in the CNC programme, and the feeder linkage structure presented in figure 1, assures the motion of the mobile elements so as their current position to (ideally) coincide with the reference position. There is no doubt that with any automated adjustment system there are different types of errors during operation that must be reduced as much as possible in occurrence, through an adequate setting of the controller units.

3.2. Defining the Transfer Functions of the System

In order to define the overall transfer function, according to the automated adjustment theory, it is necessary to take into consideration the transfer functions of each individual component.

Based on this, the Laplace transform method will be applied determining the transfer function of each component of the studied numerical axes.

For the direct current induction motor, the following ratios can be established:

$$M(t) = K_t \cdot i(t); \quad (3.1)$$

$$e(t) = K_v \cdot \omega(t); \quad (3.2)$$

$$U_b(t) = L \frac{di(t)}{dt} + Ri(t) + e(t); \quad (3.3)$$

$$M(t) = J \frac{d\omega(t)}{dt} + B\omega(t) + M_s(t); \quad (3.4)$$

$$e(t) = U_b(t) - R \cdot i(t); \quad (3.5)$$

$$P(t) = M(t) \cdot \omega(t) = e(t) \cdot i(t); \quad (3.6)$$

where:

M is the total movement produced by the motor [Nm];

i - the induced current [A];

U_b - voltage at motor terminals [V];

e - counter-electromotive force [V];

L - inductive inducer [H];

ω - motor revolutions[rad/s];

M_s - static moment [Nm];

B - coefficient of internal friction [Nms/rad];

J - motor inertia moment [kgm²];

R - resistance of inducer [Ω];

K_t - constant of motor coupling [Nm/A];

K_v - speed coefficient [Vs/rad];

P - motor power [W].

According to a relative simple calculus and making the transfer from the time variable t to the complex s variable, the following ratio is established:

$$\omega(s) = \frac{K_t U_b(s) - M_s(s)(R + Ls)}{(R + Ls)(B + Js) + K_t K_v} \quad (3.7)$$

In case of direct current servo motors with reduced inertia, used as execution elements for numerical axes, the inductance of the rotor is lower than 100 μH and it can be neglected. Thus for the revolution of the motor the following ratio is set:

$$\omega(s) = \frac{K_t U_b(s) - M_s(s)R}{RJs + RB + K_t K_v} \quad (3.8)$$

In the vast number of cases encountered in practice, the static moment is of constant value and not representing a time function, making the Laplace transform null, $M_s(s)=0$. Under such conditions the ratio (3.8) can be re-written as;

$$\omega(s) = U_b(s) \frac{K_t}{1 + \tau_m \cdot s}, \quad (3.9)$$

where τ_m is the constant of mechanical time [s], defined as follows:

$$\tau_m = \frac{RJ}{RB + K_t K_v} \quad (3.10)$$

Based on the functional layout of the speed adjustment loop, presented in figure 3.2, the ratio can be written as follows:

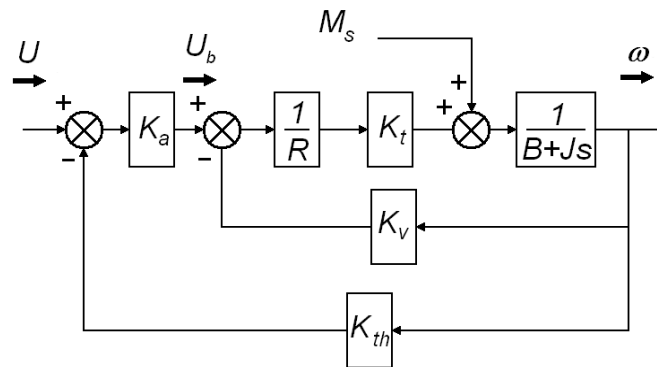


Fig. 3.2: The functional layout of the speed adjustment loop

$$\omega(s) = \frac{\alpha}{1 + \tau \cdot s} \left[U(s) \frac{K_a K_t}{RB + K_t K_v} \right], \quad (3.11)$$

where:

K_a is the constant of the power amplifier (adimensional – without dimensions)

K_{th} – the constant of the tachogenerator [Vs/rad];

U – the input voltage for the speed adjustment analog system [V];

τ - the constant of time for the loop [s], defined by:

$$\tau = \alpha \tau_m, \quad (3.12)$$

α - damping factor, defined by the ratio:

$$\alpha = \frac{1}{1 + \frac{K_a K_t K_{th}}{RB + K_t K_v}}. \quad (3.13)$$

The calculus ratio for the motor revolution becomes:

$$\omega(s) = \frac{K_1 U(s)}{1 + \tau s}, \quad (3.14)$$

for which:

$$K_1 = \frac{\alpha K_a K_t}{RB + K_t K_v} \text{ [rad/Vs]}. \quad (3.15)$$

Ratio (13) can be re-written as follows:

$$\frac{\omega(s)}{U(s)} = \frac{K_1}{1 + \tau s}. \quad (3.16)$$

As such, ratio (3.16) represents the transfer function of the speed adjustment analog system.

What follows, and taking into consideration the functional role of each component element, we can design the functional layout of the position adjustment system, according to figure 3.3.

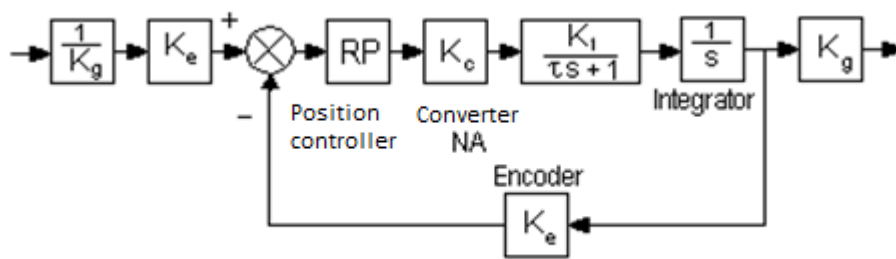


Fig. 3.3: The functional layout of the position adjustment system

In figure 3.3., are noted the additional values:

K_e –the constant of the photoelectric rotary incremental numerical transducer, hereandafter referred to as encoder and defined by the ratio:

$$K_e = \frac{N_{imp}}{2\pi} \text{ [impulses/rad]}, \quad (3.17)$$

where:

N_{imp} represents the number of impulses issued by the transducer (encoder) for a full/ complete rotation.

K_g . the amplification coefficient of the mechanical transmission, defined by the ratio:

$$K_g = \frac{ip}{2\pi} [m], \quad (3.18)$$

where i represents the transmission ratio of the redactor and p the pitch of the conducting screw [m].

K_c is conversion coefficient of the analog-to-digital conveter that indicates the value with which the output voltage needs to be adjusted at the bit input signal, defined by the ratio:

$$K_c = \frac{U}{2^{n-1}} [V/bit] \quad (3.19)$$

U represents the output voltage of the analog-to-digital conveter (the input voltage of the analog speed adjustment system), and n represents the number of bits.

3.3. Position Controller

The flow chart of the position controller is presented in figure 3.4. After making the adjustment, the output value (command) is applied at the input point of the analog-to-digital conveter and characterised by the K_c constant. The output value of the analog-to-digital conveter is represented by the U voltage, whose significance was defined above.

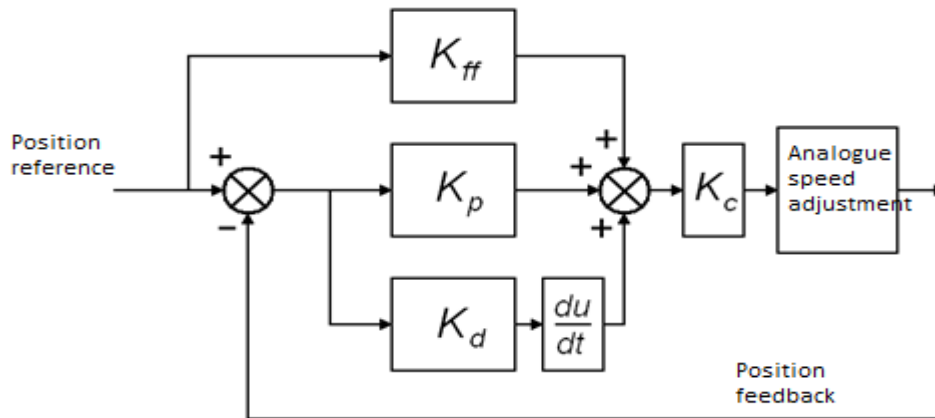


Fig. 3.4: The flow chart of the position controller

From figure 3.4, it can be observed that for the position controller, the proportional, derivative and feed-forward type of accumulative effect adjustment was proposed.

This decision was made after analysing the main types of CNC equipment adherent to the laser cutting machinery, which shows that these effects are the most encountered types for the process of position adjustment.

Furthermore, the adjustment constants that characterise the three effects (proportional, derivative and feed-forward) are accessible and can be modified directly from the operator-panel of the CNC equipment for the cutting machine.

Moreover, the preliminary research has shown that in over 80% of cases, the only adjustment effect taken into consideration was the proportional one, the rest are set at null/ zero values.

The proposed approach will later on allow, if necessary, the consideration of the integrative effect of the adjustment.

At first stage, taking into consideration only the proportional adjustment effect, the law governing it, can be noted as:

$$c_{vit} = \Delta p_{ur} \cdot (K_p \cdot K_c), \quad (3.20)$$

where:

c_{vit} is the speed command (the output value from the position controller) [V];

Δp_{ur} – follow-up error (the immediate difference between the imposed position and the current one) [m];

K_p – the constant of proportionality of the controller [bit/m];

K_c – the conversion coefficient of the analog-to-digital converter (defined above) [V/bit].

The speed command (c_{vit}) represents the analog output value that corresponds to a feed rate that leads to a follow-up error (Δp_{ur}) of 1mm. This could also be expressed with the formula:

$$c_{vit} = \frac{F \cdot U_{max}}{F_{max}}, \quad (3.21)$$

where:

F is the feed rate corresponding to the feeder work movement mode [mm/min];

F_{max} – the feed rate corresponding to a fast feeder motion [mm/min];

U_{max} – the maximum value of the voltage from the analog-to-digital converter output [V].

Taking into consideration the follow-up error of 1 mm, the formula is written:

$$K_p = \frac{F \cdot U_{max}}{F_{max}} \cdot \frac{1}{K_c}. \quad (3.22)$$

What follows, and taking into consideration the effects of derivative and feed-forward adjustment effects, ratio (20) can be re-written as follows:

$$c_{vit} = (\Delta p_{ur} \cdot K_p + \frac{\Delta p_{ur} \cdot K_d}{10 \cdot t} + \frac{K_{ff} \cdot F \cdot U_{max}}{100 \cdot F_{max}}) \cdot K_c. \quad (3.23)$$

where:

K_d is the derivative of a constant of the controller [bit·s/m];

K_{ff} – feed forward constant of the controller [bit/V].

The K_p , K_d și K_{ff} adjustment parameters taken together with K_c have the following significance:

$K_p \cdot K_c$ –the value of the command voltage in millivolts, necessary for a follow-up error of 1 mm;

$K_d \cdot K_c$ –analog voltage (in millivolts) corresponding to a 1 mm change for the follow-up error of 10 milliseconds;

$K_{ff} \cdot K_c$ –the percentage variation (%) of the analog voltage given by the programmed feed rate.

3.4. The Model for Forces and Moments of Resistance

In order to establish the forces and moments of resistance, the layout presented below will represent a starting point (fig. 3.5).

The notations from the figure represent:

J_m – the moment of inertia of the electric motor [kgm²];

J_{Z1} – the moment of inertia of the cogwheel 1 (pinion) [kgm²];

J_{Z2} – the moment of inertia of the cogwheel 2 [kgm²];

J_{sb} – the moment of inertia of the screw [kgm²];

v – the linear speed of the load [m/s];
 a – the linear acceleration of the load [m/s²];

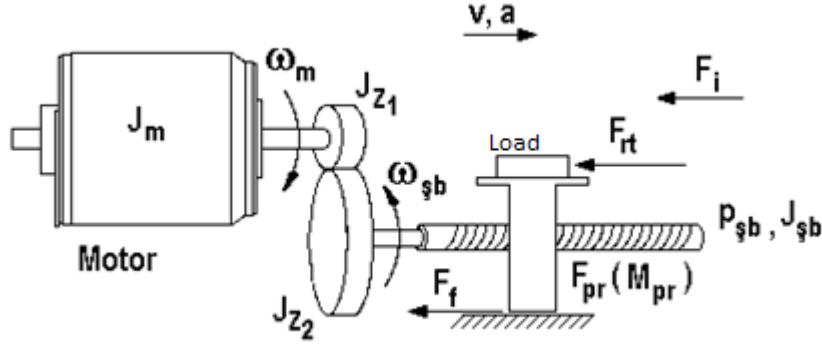


Fig. 3.5: Layout used to calculate the forces and moments of resistance

ω_m – angular velocity of the motor [rad/s];
 ω_{sb} – angular velocity of the screw [rad/s];
 F_{rt} – technological resistance force [N];
 F_i – force of inertia [N];
 F_f – friction force [N];
 F_{pr} – nut pre-clamping force [N];
 M_{pr} – nut pre-clamping moment [Nm];
 p_{sb} – screw pitch [m].

The necessary static moment, reported to the crankshaft of the motor, is calculated from the condition of power equality at crankshaft level (rotary motion) and load value (translational motion), and considering the gear transmission and the nut-screw transmission.

$$M_{st} \omega_M = \frac{F_t v_L}{\eta_t}, \quad (3.24)$$

where:

M_{st} is the necessary static moment of the crankshaft [Nm];
 F_t – the total value of the force of resistance on the direction of the axis [N];
 η_t – the total performance of the mechanical transmissions

It can be written as follows:

$$F_t = F_{rt} + F_i + F_{fr} + F_{pr} = F_{rt} + F_{pr} + m_s(a + \mu g), \quad (3.25)$$

where:

m is the total mass of the load found in motion [kg];
 μ - the friction coefficient within guards;

For the η_t value there is a ratio:

where

η_{ang} is the performance of the gear transmission (will be considered $\eta_{ang} = 0.9$)
 η_{sb} – the performance of the ballscrew (will be considered $\eta_{sb} = 0.9$)

Based on these considerations, for M_{st} , the result is:

$$M_{st} = \frac{[F_{rt} + F_{pr} + m_s(\mu + ag)]v_L}{\omega_M \eta_{ang} \eta_{sb}}. \quad (3.26)$$

Between the angular velocity of the screw and the linear velocity of the load, the following ratio is noted:

$$\frac{v_L}{\omega_{sb}} = \frac{P_{sb}}{2\pi}. \quad (3.27)$$

The transfer ratio for gear transmission is:

$$i = \frac{\omega_M}{\omega_{sb}}, \quad (3.28)$$

so:

$$\frac{v_L}{\omega_M} = \frac{P_{sb}}{2\pi i}. \quad (3.29)$$

By replacing the formula presented above in the (3.26) ratio the result is:

$$M_{st} = \frac{[F_{rt} + F_{pr} + m_s(a + \mu g)]P_{sb}}{2\pi i \eta_{ang} \eta_{sb}}, \quad (3.30)$$

or if we know the value of M_{pr} instead of F_{pr} :

$$M_{st} = \frac{[F_{rt} + m_s(a + \mu g)]P_{sb}}{2\pi i \eta_{ang} \eta_{sb}} + M_{pr}. \quad (3.31)$$

Note: In case the values of F_{pr} or M_{pr} are not known, the following estimation can be made:

$$F_{pr} = \frac{1}{3}(F_{rt} + F_i + F_{fr}) = \frac{1}{3}[F_{rt} + m_s(a + \mu g)]. \quad (3.32)$$

The necessary dynamic moment (reduced at crankshaft of the motor) is calculated using the ratio:

$$M_d = J_t \cdot \varepsilon_M, \quad (3.33)$$

where:

J_t is the total equivalent moment of inertia reduced at motor crankshaft [kgm^2];

ε_M –the angular velocity of the motor [rad/s^2].

What follows is a calculus model for J_t . In order to do so, the kinetic energy of bodies found in rotary and translation motion will be equalised with the kinetic energy of an equivalent body, in rotary motion with an angular velocity of the motor crankshaft, having the moment of inertia equal to the value of J_t :

$$\frac{J_t \omega_M^2}{2} = \frac{J_M \omega_M^2}{2} + \frac{J_{Z_1} \omega_M^2}{2} + \frac{J_{Z_2} \omega_{sb}^2}{2} + \frac{J_{sb} \omega_{sb}^2}{2} + \frac{m_s v_L^2}{2}. \quad (3.34)$$

Taking into consideration the transfer ratio of the transmission and of ratio (3.27), the formula becomes:

$$J_t = J_M + J_{Z_1} + \frac{J_{Z_2}}{i^2} + \frac{J_{sb}}{i^2} + m_s \left(\frac{p}{2\pi i} \right)^2. \quad (3.35)$$

For the calculus of the moment of inertia adherent to the cogwheel and of the screw (considered as cylinder shaped parts), the ratio is presented:

$$J = mr^2 = \rho Vr^2 = \rho L \pi r^2 \cdot r^2 = \frac{1}{16} \rho L \pi d^4, \quad (3.36)$$

where:

m –mass of the body [kg];

r,d –the radius and respectively the diameter of the body [m];

L –length of the body [m];

ρ - density of the body [kg/m³], for steel $\rho=7800$ kg/m³

Adherent to the ballscrew, the exterior diameter will be taken into consideration for the d value and for L, the total length of the race, plus the bearing length must be taken into consideration.

For the cogwheel (with straight coggings) the diameter-division value will be taken into consideration for the d value, and for L, the width of the cogging, as follows:

$$d = m_n \cdot Z; \quad (3.37)$$

$$L = \psi_d \cdot m_n \cdot Z_1 + 1.5 \cdot m_n \text{ for pinion } (Z_1); \quad (3.38)$$

$$L = \psi_d \cdot m_n \cdot Z_1 \text{ for cogwheel } (Z_2), \quad (3.39)$$

where:

ψ_d –the width coefficient of cloggings

The angular velocity is calculated taking into consideration the ratio:

$$\frac{a_L}{\varepsilon_{sb}} = \frac{p_{sb}}{2\pi} \quad (3.40)$$

and the fact that:

$$\varepsilon_M = \varepsilon_{sb} i. \quad (3.41)$$

It results:

$$\varepsilon_M = \frac{2\pi a_L}{p_{sb}} i. \quad (3.42)$$

The motor must be chosen so as the moment developed during the acceleration period (M_a) to be, at least equal to the sum of the static and dynamic moment:

$$M_a = M_{st} + M_d, \quad (3.43)$$

and during the constant speed run, the developed moment (M_{ct}) must be, at least equal to the static moment:

$$M_{ct} = M_{st}. \quad (3.44)$$

3.5. Conclusions

Within this present chapter the relations that form the basis of a mathematical modelling for the feeder linkages were presented, linkages that are a component of laser cutting machines with numerical control.

This forward linkage is equivalent to the motion control system, with an exterior position adjustment loop and internal speed adjustment loop. As execution element, the direct current servo motor was taken into consideration. This motion control system was set up using the continuous variable transfer functions.

Based on the preliminary experimental research that implied the study and analysis of a large number of numerical control equipments that are part of a laser cutting machine with numerical control, a structure for the position controller was proposed and the main corresponding adjustment parameters were defined together with their physical significance.

The main objective of the executed and documented research, was to set up the position controller, using certain parameters, accessible to the user from the command panel of the machine (operator panel). In consequence, each of the defined parameters (constant of proportionality, derivative of a constant and the feed-forward controller) can be easily adjusted by the operator for most of the numerical control equipment with laser cutting machinery. Furthermore, by explaining the physical significance of the values that intervene with the calculus formula of these parameters certain equivalences can be set between the constant values defined within and those accessible from the operator-panel of some numerical control equipments, in case these do not coincide.

As such, in the following chapter, by means of simulation examples, the influence of these adjustment parameters applied to different operational functions of the equipment will be studied and recommendation strategies will be established in order to improve the processing precision, based on the adjustment of the position controller.

Also within this chapter, it was presented the calculus relations necessary to determine the forces and moments of resistance that occur during the processes and that will later on form the basis of the presented simulation study.

Chapter 4

The Simulation Study of Feeder Linkages' Behaviour Comprised by a Laser Cutting Machine with a Numerical Control Structure, During Different Operational Modes

4.1. Initial Data

The basis of the simulation study was conducted using the features of the MAZAK ST-X48 MkII cutting laser machine with numerical control.

The equipment has three numerical controlled axes (X, Y, Z), the execution element for each axis is a direct current servo motor of $\alpha 6/3000$ GE Fanuc type and with the following values and parameters:

- moment developed by the motor $M = 6 \text{ Nm}$;
- the maximum moment developed by the motor $M_{\max} = 56 \text{ Nm}$;
- root mean square (RMS) of the induced current $I = 10 \text{ A}$;
- the maximum admissible value of the current $I_{\max} = 132 \text{ A}$;
- maximum revolution of the motor $n_{\max} = 4000 \text{ rot/min}$;
- coefficient of viscous friction $B = 0.75 \cdot 10^{-4} \text{ Nms/rad}$;
- moment of inertia of the motor $J = 0.26 \cdot 10^{-2} \text{ kgm}^2$;

- resistance of the inducer $R = 0.18 \Omega$;
- constant of motor coupling $K_t = 0.6 \text{ Nm/A}$;
- speed coefficient $K_v = 0.2 \text{ Vs/rad}$;
- mechanical time constant $\tau_m = 0.004 \text{ s}$;
- constant of the tachogenerator $K_{th} = 0.007 \text{ Vs/rad}$;
- maximum voltage at the analog-to-digital convertor output (the input voltage for the speed adjustment system) $U_{\max} = 10 \text{ V}$;
- number of bits for the analog-to-digital convertor $n = 16$;
- conversion coefficient of the analog-to-digital convertor $K_c = 0.00030518 \text{ V/bit}$;
- reductor transmission ratio $i = 1$ (there are no reductors);
- constant of the photoelectric rotary incremental numerical transducer (encoder) $K_e = 2500/2\pi$ impulses/rad;
- pitch of conductive screw for each axes $p_{sb} = 0.01 \text{ m}$;
- coefficient of the mechanical transmission amplification $K_g = 0.01/2\pi \text{ m}$.

In order to calculate the value of the K_a power amplification constant, we must calculate the engine's terminal voltage using the ratio:

$$U_b = K_v \omega + RI, \quad (4.1)$$

where ω represents the angular velocity of the engine, calculated using:

$$\omega = \frac{\pi n}{30} [\text{rad/s}]. \quad (4.2)$$

Imposing the maximum working values for the n (4000 rot/min) revolution and I (10 A) induced current, the maximum terminal voltage is obtained $U_b = 85.57 \text{ V}$.

As such, the K_a constant of power amplification can be calculated as follows:

$$K_a = \frac{U_b}{U_{\max}} = \frac{85.57}{10} = 8.557. \quad (4.3)$$

4.3. The calculus of forces and moments of resistance for the X axis (displacement linkages for table movement)

The stages foreseen in chapter 3 will be followed closely using the following features of the machine:

- maximum revolution of the electric motor $n_{\max} = 4000 \text{ rot/min}$;
- direct coupling of the motor to the axle of the ball screw (no gearing);
- ballscrew pitch $p_{sb} = 10 \text{ mm} = 10 \cdot 10^{-3} \text{ m}$;
- diameter of the ball screw $d_{sb} = 25 \text{ mm} = 25 \cdot 10^{-3} \text{ m}$;
- the total length of the ball screw $l_{sb} = 2500 \text{ mm} = 2.5 \text{ m}$;
- pre-clamping moment of the ball screw (estimated) $M_{pr} = 0.5 \text{ Nm}$;
- the maximum linear velocity during the fast approachment phase, respectively fast retreat $v_R = 24 \text{ m/min} = 0.4 \text{ m/s}$;
- technical maximum speed $v_T = 15 \text{ m/min} = 0.25 \text{ m/s}$.

The angular acceleration of the motor can be determined with the help of:

$$\varepsilon_m = \frac{M}{J_m} = \frac{6}{0.0026} = 2307.6923 \text{ rad/s}^2. \quad (4.9)$$

The linear acceleration can be calculated using:

$$a = \frac{\varepsilon_m}{2\pi} \cdot i \cdot p_{sb} = \frac{2307.6923}{2 \cdot 3.1415} \cdot 1 \cdot \frac{10}{1000} = 3.6728 \text{ m/s}^2. \quad (4.10)$$

As such, based on the formula presented above, the following values were taken into consideration:

- maximum linear acceleration during the fast approachment phase, respectively fast retreat $a_{AR} = a_{RR} = 1.5 \text{ m/s}^2$ (calculated value, 3.6728 m/s^2 was considered too high);
- maximum linear acceleration during the technical advancement phase $a_{AT} = 0.25 \text{ m/s}^2$.

Other data to be considered:

- the total mass taken into consideration (the value of the table and those admitted on the table) $m_s = 400 \text{ kg}$;
- gear friction coefficient $\mu = 0.01$ (a cover value was taken into account, considering the rolling parts - ball bushings);
- technical resistance force during the fast approachment phase $F_{rt_AR} = 0 \text{ N}$;
- technological resistance force during the technical advancement phase $F_{rt_AT} = 0$.

Practically, for the laser beam cutting process there are no technical forces of resistance.

The static moment during the fast approachment phase:

$$M_{st_AR} = \frac{[F_{rt_AR} + m_s(a_{AR} + \mu g)]p_{sb}}{2\pi\eta_{sb}} + M_{pr} = \quad (4.11)$$

$$\frac{[0 + 400(1.5 + 0.01 \cdot 9.81)]10 \cdot 10^{-3}}{2\pi \cdot 0.9} + 0.5 = 1.6304 \text{ Nm.}$$

The static moment during the fast retreat phase has the same value for M_{st_RR} and opposite sign.

The static moment during the technical advancement phase:

$$M_{st_AT} = \frac{[F_{rt_AT} + m_s(a_{AT} + \mu g)]p_{sb}}{2\pi\eta_{sb}} + M_{pr} = \quad (4.12)$$

$$\frac{[0 + 400(0.25 + 0.01 \cdot 9.81)]10 \cdot 10^{-3}}{2\pi \cdot 0.9} + 0.5 = 0.7462 \text{ Nm.}$$

According to the ratios established in the previous chapter, the total moment of inertia is of:

$$J_t = J_M + J_{sb} + J_C + m_{sb} \left(\frac{p_{sb}}{2\pi} \right)^2. \quad (4.13)$$

It can be observed that, in addition it was taken into consideration the moment of inertia of the coupling between the screw and the motor, $J_c = 200 \cdot 10^{-6} \text{ kgm}^2$ (catalogue data).

According to ratio (3.36) for the moment of inertia of the screw it can be determined:

$$J_{sb} = \frac{1}{16} \rho L_{sb} \pi d_{sb}^4 = \frac{1}{16} \cdot 7800 \cdot 2.5 \cdot \pi \cdot (25 \cdot 10^{-3})^4 = 14.9563 \cdot 10^{-4} \text{ kgm}^2. \quad (4.14)$$

The total moment of inertia becomes:

$$J_t = J_M + J_{sb} + J_C + m_s \left(\frac{P_{sb}}{2\pi} \right)^2 = 0.26 \cdot 10^{-2} + 14.9563 \cdot 10^{-4} \quad (4.15)$$

$$+ 200 \cdot 10^{-6} + 400 \left(\frac{10 \cdot 10^{-3}}{2\pi} \right)^2 = 53.0884 \cdot 10^{-4} \text{ kgm}^2.$$

Taking into account the total value of the moment of inertia J_t , the maximum angular acceleration of the motor can be re-calculated, taking into consideration the actuated load, so as:

$$\varepsilon_{\max_m} = \frac{M_n}{J_t} = \frac{6}{53.0884 \cdot 10^{-4}} = 1130.1903 \text{ rad/s}^2. \quad (4.16)$$

It must be verified that this angular acceleration does not lead to a linear acceleration higher than that imposed of 1.5 m/s^2 by using the relation:

$$a = \frac{\varepsilon_m}{2\pi} \cdot i \cdot p_{sb} = \frac{1130.1903}{2 \cdot 3.1415} \cdot 1 \cdot \frac{10}{1000} = 1.7987 \text{ m/s}^2 > 1.5 \text{ m/s}^2. \quad (4.17)$$

Under these conditions, the angular acceleration is re-calculated limiting a linear acceleration of 1.5 m/s^2 , according to the relation:

$$\varepsilon_m = \frac{a \cdot 2\pi}{i \cdot p_{sb}} = \frac{1.5 \cdot 2\pi}{1 \cdot 10 \cdot 10^{-3}} = 942.4777 \text{ rad/s}^2. \quad (4.18)$$

As such, the angular acceleration of the motor during the fast approachment phase, respectively fast retreat will have the $\varepsilon_{m_AR} = \varepsilon_{\max_m} = 942.4777 \text{ rad/s}^2$ value.

For the angular acceleration of the motor during the technical advancement phase, the following relation can be written down:

$$\varepsilon_{M_AT} = \frac{2\pi a_{AT}}{P_{sb}} = \frac{2\pi \cdot 0.25}{10 \cdot 10^{-3}} = 157.0796 \text{ rad/s}^2. \quad (4.19)$$

For the dynamic moment activated during the fast approachment phase, respectively fast retreat, we have the ratio:

$$M_{d_AR} = -M_{d_RR} = J_t \cdot \varepsilon_{M_AR} = 53.0884 \cdot 10^{-4} \cdot 942.4777 = 5.0034 \text{ Nm}. \quad (4.20)$$

For the dynamic moment during the technical advancement phase we have:

$$M_{d_AT} = J_t \cdot \varepsilon_{M_AT} = 53.0884 \cdot 10^{-4} \cdot 157.0796 = 0.8339 \text{ Nm}. \quad (4.21)$$

Adding the static and dynamic moments for the quick advancement modes and technical advancement mode, we have:

$$M_{tot_AR} = -M_{tot_RR} = M_{st_AR} + M_{d_AR} = 1.6304 + 5.0034 = 6.6338 \text{ Nm}. \quad (4.22)$$

respectively

For the feed rate corresponding to a work advancement motion, necessary in the calculus of the K_p value, the $F = 15000 \text{ mm/min}$ value was taken into consideration (taken from the manual of the machine).

In figures 4.5-4.7 are presented the simulation rates of the kinematic reference values (position, speed, acceleration):

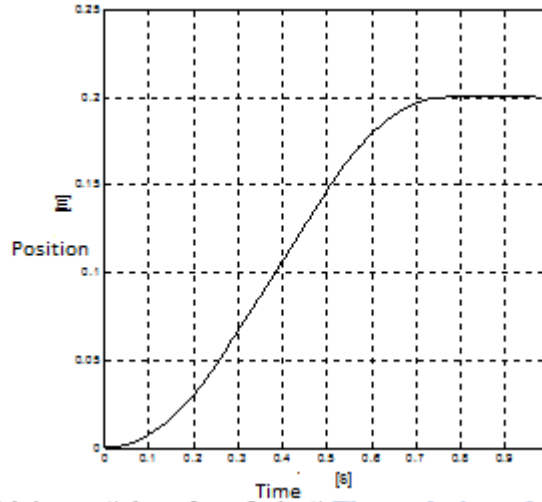


Fig. 4.5: The evolution of the position as reference value

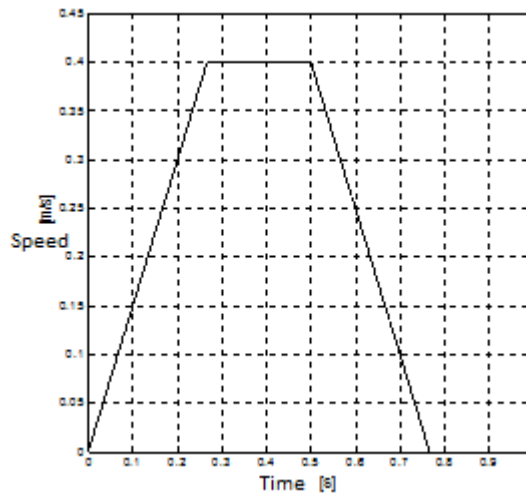


Fig. 4.6: The evolution of speed as reference value

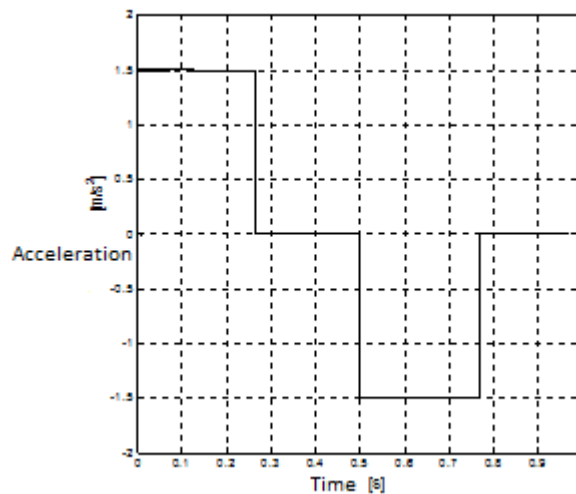


Fig. 4.7: The evolution of acceleration as reference value

In figures 4.8 and 4.9 are presented the simulated values of output linkages (speed and acceleration):

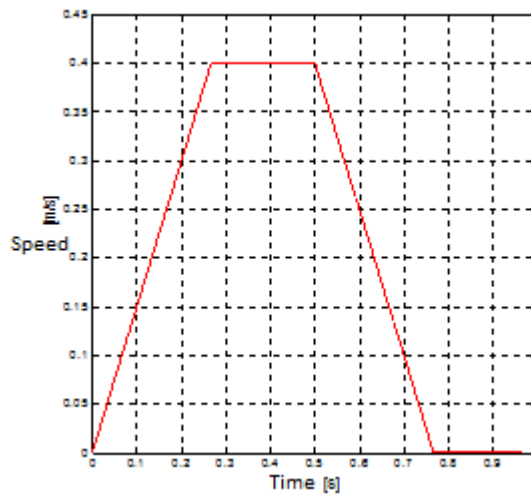


Fig. 4.8: The evolution of speed as output value

Instead of position as output value, it was opted for the evolution of positioning error, as a difference between the reference position and output position (fig 4.10):

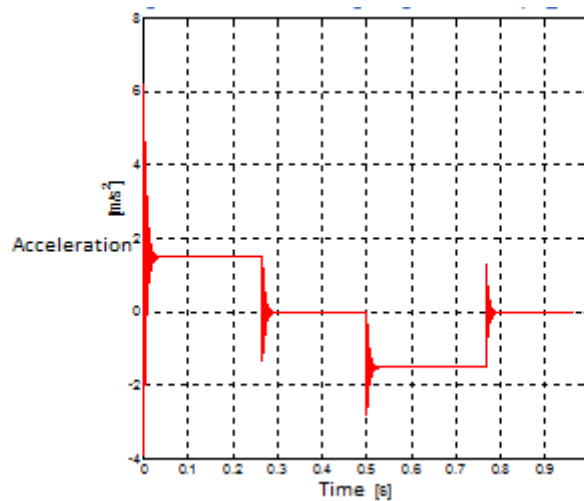


Fig. 4.9: The evolution of acceleration as output value

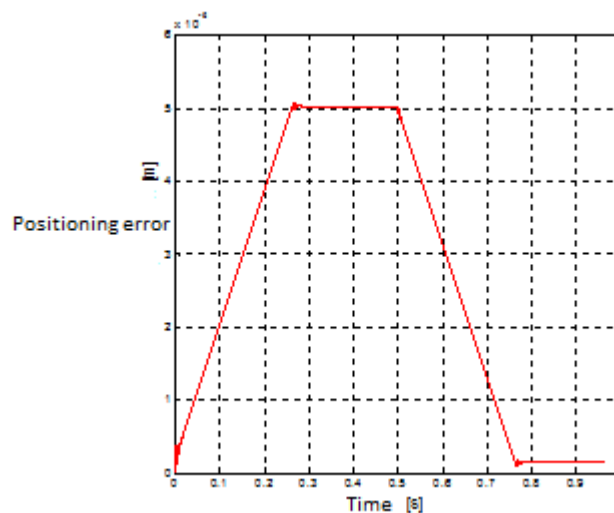


Fig. 4.10: The evolution of positioning error

The final value of the positioning error is of $0.14314 \mu\text{m}$, a relatively low value for these types of equipments and processings. However, the evolution of acceleration as output value, presented in figure 4.9 is completely non-conformant and presented pronounced oscillations with a range between -3.9 m/s^2 and 6.2 m/s^2 , that can lead to serious defects or even damages.

As such, it can be preliminary concluded that within this phase, the system's behaviour is non-compling, especially from a dynamic point of view.

For a better understanding of the system's dynamic behaviour, an input signal with a stage variation will be applied at the acces point, in order to obtain a stage variation of the angular velocity ω for the motor, with a maximum value of 1 rad/s .

Starting from the (3.27) ratio, it can be deducted:

$$\frac{v}{\omega} = \frac{p_{sb}}{2\pi} . \quad (4.37)$$

Based on the relation mentioned above, the linear speed can be calculated in order to be applied at the input of the system, with a stage like deviation that results in a ω stage variation with a maximum value of 1 rad/s .

$$v = \frac{p_{sb} \cdot \omega}{2\pi} = \frac{10 \cdot 10^{-3} \cdot 1}{2\pi} = 0.0157 \text{ m/s} . \quad (4.38)$$

In figure 4.11 are presented, on the same graphic, the speed stage input signals (black colour) and speed output signals (red colour).

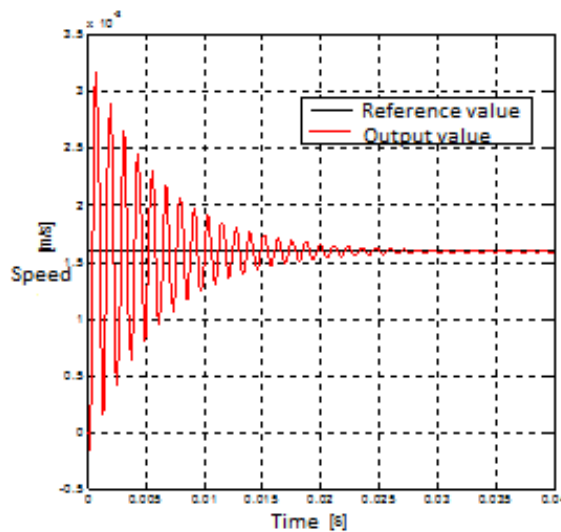


Fig. 4.11: Speed output reference signals

From the figure presented above it can be observed that the output signal presents very powerfull oscilacions. According to the literature in the field, the reduction of such oscilacions can be made through:

- the reduction of the controller's constant of proportionality K_p , but in the present case it can lead to an increase of positioning error;
- the introduction of a derivative effect, by using a K_d derivative of a constant which is not null.

For this case, it was opted for the second solution. Based on a trial-and-error process facilitated by means of the simulation study, it has been noticed that a corresponding value for the derivative constant is of $K_d = 10 \text{ bit}\cdot\text{s/m}$.

In figure 4.12 are presented, in the same graphic, the stage speed input signals (black colour) and the speed output signals (red colour), accumulating the proportional effect and the derivative one for the position controller.

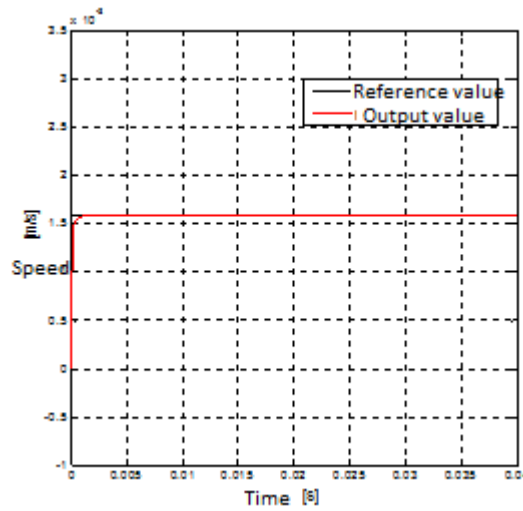


Fig. 4.12: Reference and speed output signals, after accumulating the proportional and derivative effects

It can be observed that the two signals are almost identical, with a slight delay, lower than 2 milliseconds for the output signal, so practically insignificant. Moreover, the output signal does not present any other oscillations.

It can be concluded that, according to the present case, the studied system has an appropriate dynamic behaviour.

Coming back to the input signal (position, speed and acceleration), specific to the uniaxial fast positioning mode, in figures 4.13-4.15 are presented the evolutions of output values, after introducing the derivative effect.

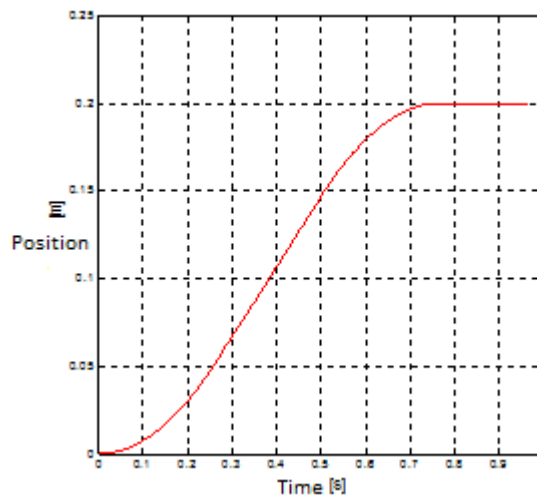


Fig. 4.13: The evolution of the position as output value after introducing a derivative effect

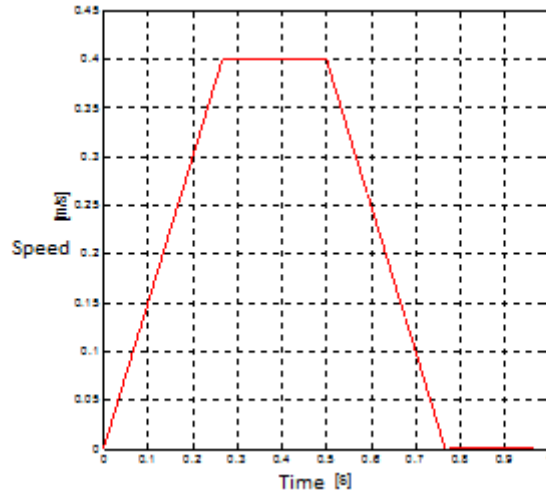


Fig. 4.14: The evolution of speed as output value after introducing the derivative effect

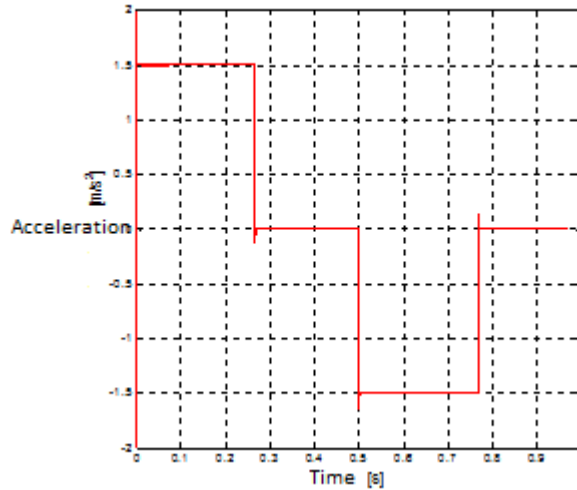


Fig. 4.15: The evolution of acceleration as output value after introducing the derivative effect

It can be observed that the acceleration oscillation as output value is more reduced in this case.

In figure 4.16 is presented the evolution of the positioning error when accumulating the two effects, the proportional and derivative one.

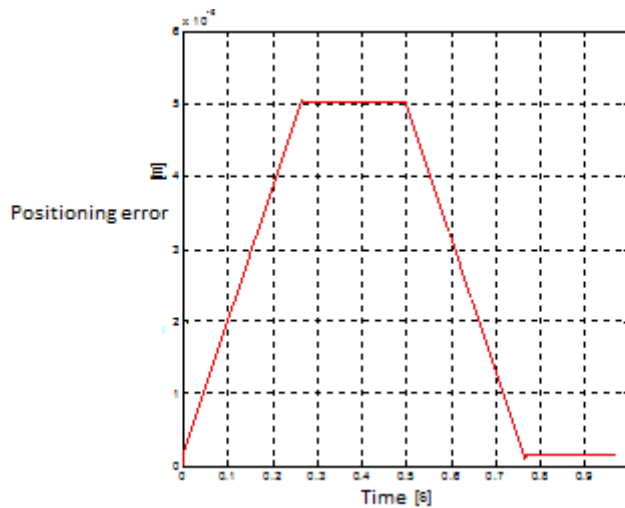


Fig. 4.16: The evolution of the positioning error after introducing the derivative effect

It can be observed that the changes occurred for positioning error are insignificant, the final value is equal to the previous case, 0.14314 μm .

In figure 4.17 is presented the evolution of the current passing through the induction motor.

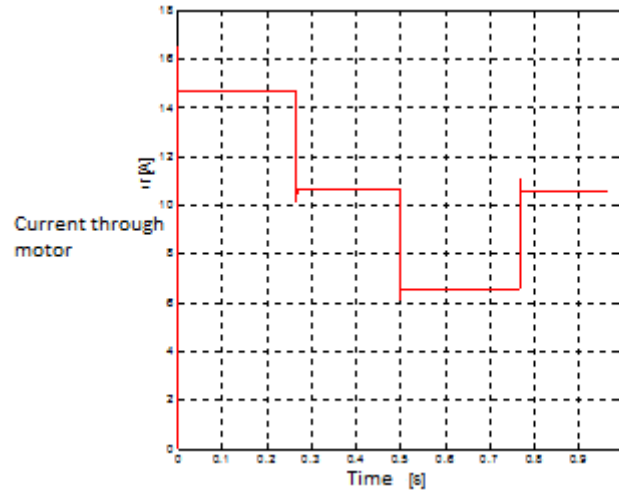


Fig. 4.17: The evolution of the current through the induction motor

It can be observed that the current's evolution is similar (from a quality point of view) to the evolution of the acceleration; the maximum values do not surpass the admissible maximum value of $I_{\text{max}} = 132 \text{ A}$.

4.6 Simulation Study of the Biaxial Outlining

4.6.1. Interpolation Algorithm for the Techniques Using Reference Words

The interpolation conducted with the help of reference words techniques presupposes generating reference values for the two movement axes, taking the form of codified values for a certain code (usually a binary code) at equal periods of time for the sampling frame of the CNC equipment.

Thereby, in order to generate a circular motion (full circle) for the XOY plan using a circular interpolation algorithm, the main condition is to maintain the feed rate at a constant value, on the F trajectory. As a correspondent, the feed rate for the X and F axes, F_x respectively F_y , can be expressed according to the following ratio:

$$\begin{cases} F_x = F \sin \theta(t); \\ F_y = F \cos \theta(t), \end{cases} \quad (4.39)$$

where

$\theta(t)$ is peak angle at t moment

The dependency between the $\theta(t)$ angle, the feed rate on the trajectory, angular speed and the radius of the circle can be expressed with the relation:

$$\theta(t) = \frac{F \cdot t}{R} \quad (4.40)$$

and

$$F = \omega \cdot R = \frac{2\pi}{T} \cdot R, \quad (4.41)$$

where

R – circle radius [m];

T – the time necessary to generate a full circle (time frame) [s].

ω –angular speed [rad/s].

The (4.41) relation results to:

$$\omega = \frac{2\pi}{T} = \frac{F}{R}. \quad (4.42)$$

The circular trajectory is usually approximated through small size linear stage segments. The number of such stages must be optimised so as any deviation from the circular trajectory must not surpass the minimum increment linear movement of the equipment (1 BLU).

In figure 4.18 is presented, in graphic form, the relation between the two successive points on the interpolated circular arc.

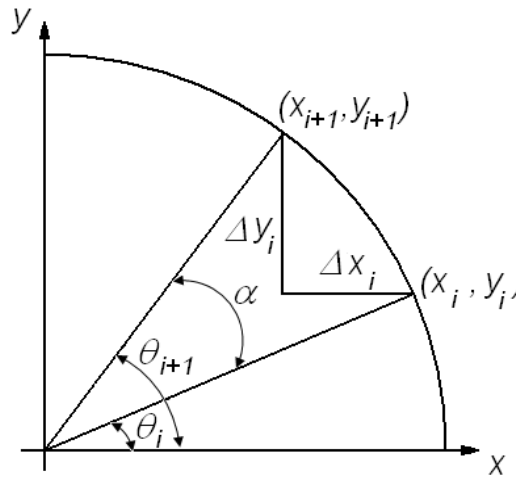


Fig. 4.18: The circular interpolation used within the reference word technique

Based on figure 4.18 the following relations can be set:

$$\begin{cases} \cos \theta(i+1) = A \cos \theta(i) - B \sin \theta(i); \\ \sin \theta(i+1) = A \sin \theta(i) + B \cos \theta(i), \end{cases} \quad (4.43)$$

where:

$$\begin{aligned} A &= \cos \alpha, & B &= \sin \alpha; \\ \theta(i+1) &= \theta(i) + \alpha, \end{aligned} \quad (4.44)$$

And α is the angular displacement increment of the interpolation algorithm [degrees].

The coordinates of the final point for the line segment used in the approximation (x_{i+1}, y_{i+1}) process, can be estimated with the help of:

$$\begin{cases} x(i+1) = R \cos \theta(i+1); \\ y(i+1) = R \sin \theta(i+1). \end{cases} \quad (4.45)$$

From (4.43) and (4.45) the following relations can be written to allow the calculus of the current point coordinates $i+1$, based on the coordinates of the previous i point:

$$\begin{cases} x(i+1) = Ax(i) - By(i); \\ y(i+1) = Ay(i) + Bx(i). \end{cases} \quad (4.46)$$

The dependency relation between the linear movement increments for each axes, Δx_i , Δy_i and the line segment coordinates can be expressed through:

$$\begin{cases} \Delta x(i) = x(i+1) - x(i) = (A-1)x(i) - By(i); \\ \Delta y(i) = y(i+1) - y(i) = (A-1)y(i) + Bx(i). \end{cases} \quad (4.47)$$

The speed for each axes, F_x , F_y can be established through relation:

$$\begin{cases} F_x(i) = F \frac{\Delta x(i)}{\Delta s(i)}; \\ F_y(i) = F \frac{\Delta y(i)}{\Delta s(i)}, \end{cases} \quad (4.48)$$

where:

$$\Delta s(i) = \sqrt{(\Delta x(i))^2 + (\Delta y(i))^2}. \quad (4.49)$$

By combining the two relations presented at (4.43) and (4.45) the result is:

$$\begin{cases} x(i+1) = R[A \cos \theta(i) - B \sin \theta(i)]; \\ y(i+1) = R[A \sin \theta(i) + B \cos \theta(i)]. \end{cases} \quad (4.50)$$

Taking into consideration the (4.40) relation and the digital-interactive interpolation algorithm for the T_i time, the relation states:

$$\theta(i) = \frac{F}{R} T_i. \quad (4.51)$$

Furthermore, the following relations can be set:

$$T_i = i \cdot T_s \quad (4.52)$$

and

$$T = n \cdot T_s, \quad (4.53)$$

Where

T_s represents the sampling period [s];

k –number of samples at moment T_k ;

n –total number of samples.

As such, the (4.50) relation can be re-written as:

$$\begin{cases} x(i+1) = R[A \cos(2\pi \cdot \frac{i}{n}) - B \sin(2\pi \cdot \frac{i}{n})]; \\ y(i+1) = R[A \sin(2\pi \cdot \frac{i}{n}) + B \cos(2\pi \cdot \frac{i}{n})]. \end{cases} \quad (4.54)$$

By combining the (4.41) and (4.53) relations, the total number of samples can be calculated as:

$$n = \frac{2\pi \cdot R}{F \cdot T_s}. \quad (4.55)$$

As a consequence, the (4.54) relation can be re-written as:

$$\begin{cases} x(i+1) = R[A \cos(\frac{F \cdot T_s}{R} \cdot i) - B \sin(\frac{F \cdot T_s}{R} \cdot i)]; \\ y(i+1) = R[A \sin(\frac{F \cdot T_s}{R} \cdot i) + B \cos(\frac{F \cdot T_s}{R} \cdot i)]. \end{cases} \quad (4.56)$$

The angular displacement increment θ_{incr} can be calculated with:

$$\theta_{incr} = \frac{2\pi}{T} \cdot T_s = \frac{F}{R} \cdot T_s, \quad (4.57)$$

and the linear displacement increment l_{incr} with:

$$l_{incr} = 2R \cdot \frac{\theta_{incr}}{2\pi} = \frac{F}{\pi} T_s, \quad (4.58)$$

relation that expresses the dependency between the linear displacement increment from the sampling period of the system and the feed rate on the trajectory.

The method presented above is dependent on the values of the angular displacement increment for the interpolation algorithm, α , as well as the approximation method for values A and B.

4.6.4 Simulation Chart

In order to simulate the behaviour of the feeder linkages for the biaxial outlining, the chart presented in figure 4.20 was created using the Matlab & Simulink software package.

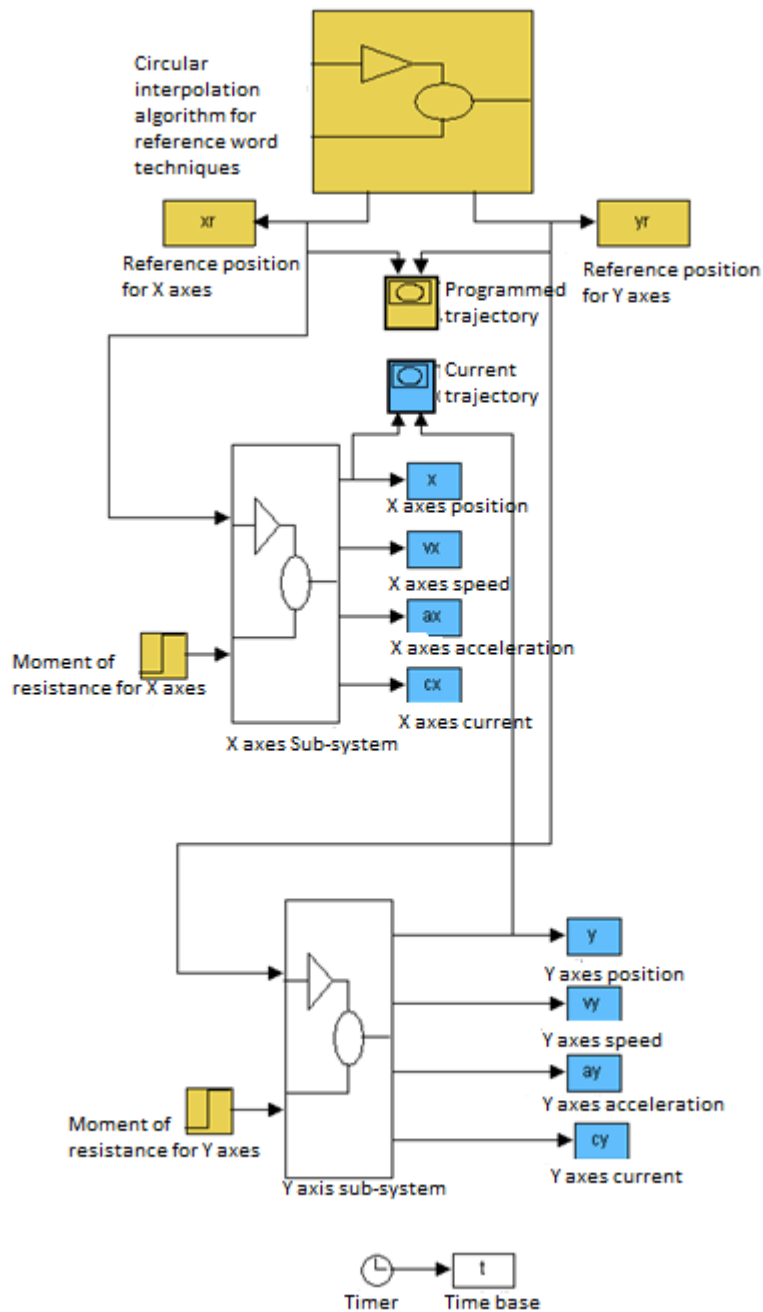


Fig. 4.20: Chart presenting the simulated behaviour of the biaxial outlining mode

The chart presented in figure 4.20 includes the sub-system called "circular interpolation algorithm for reference words techniques" that materialises this algorithm, generating reference values for the two motion axes, according to the (4.56) relation whose structure is presented in figure 4.21.

In order to generate the sine and cosine sampling functions, specific blocks were used. In figure 4.22 is exemplified the configuration mode of a cosine sampling function for the X axis. The amplitude of the function is equal to the circle radius, indicated by "Rad", the total number of n samples- calculated based on relation (4.55), and rounded up to the nearest whole number by using the "round" Matlab function. The difference between the sine and cosine signal was materialised based on the entry of a certain number of samples, referred to as "offset samples" and whose number, N_{offset} , was calculated using the relation:

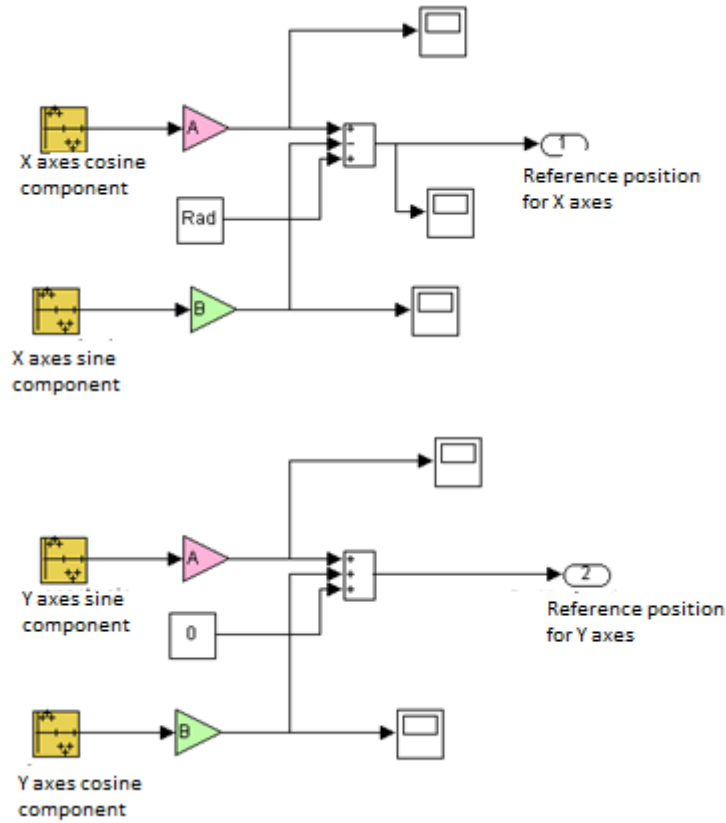


Fig. 4.21: The sub-system that materialises the circular interpolation algorithm for techniques using reference words

$$N_{offset} = -\frac{\frac{\pi}{2} \cdot \text{round}(n)}{2\pi} \quad (4.69)$$

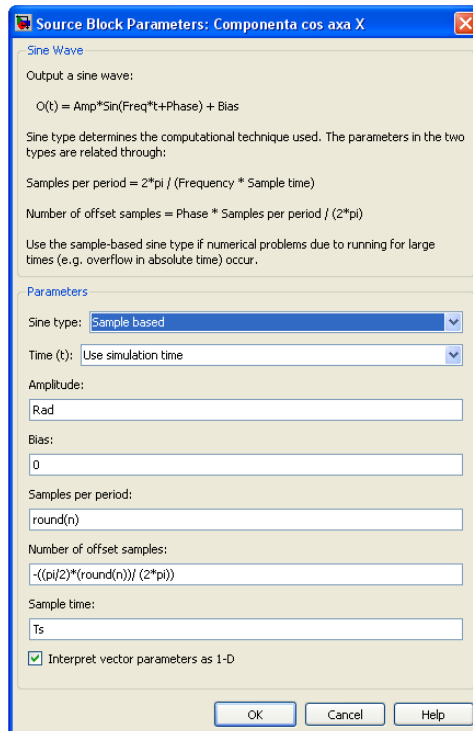


Fig. 4.22: The configuration of the sample cosine function for the X axis

4.6.5 Simulation Exemples

It was considered that the the two feeder linkages, for the X and Y axes, are identical from the actuation motor point of view and of the adjustment parameters. The difference between them consisting only in the technical moments of resistance during the advance, as presented in table 4.2.

A cutting process simulation was concluded for a full circle. As a first step, the data used for the simulation were:

- the technical feed rate for the circular trajectory $F = 2 \text{ m/min} = 2000 \text{ mm/min}$;
- circle radius $R_{ad} = 0.03 \text{ m} = 30 \text{ mm}$
- the adjustment parameters, identical for both axes $K_p = 2730.7 \text{ bit/m}$, $K_d = 0 \text{ bit}\cdot\text{s/m}$, $K_{ff} = 0$.

Due to the adjustments made at the technical feed rate level taken into consideration, the value of the constant of proportionality for the position controller was changed in comparison to the uniaxial quick movement. Its' value is calculated according to the relation below:

$$K_p = \frac{F \cdot U_{\max}}{F_{\max}} \cdot \frac{1}{K_c} = \frac{2000 \cdot 10}{24000} \cdot \frac{1}{0.00030518} = 2730.7 \text{ bit / m} . \quad (4.70)$$

The evolution of the reference positions, for the two axes, X and Y, is presented in figures 4.23 and 4.24

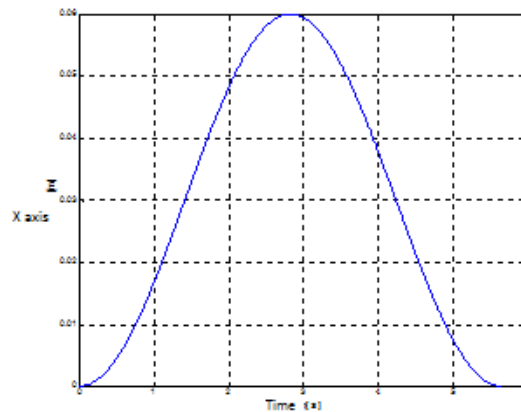


Fig. 4.23:) The evolution of the reference position (X axis)

In figure 4.25 are presented the reference and current trajectories resulted from combining the position signals of the two axes. It is observed, from the chart presented in the figure, that the two trajectories are practically heteronomous and it is impossible to highlight the deviations occurred between them.

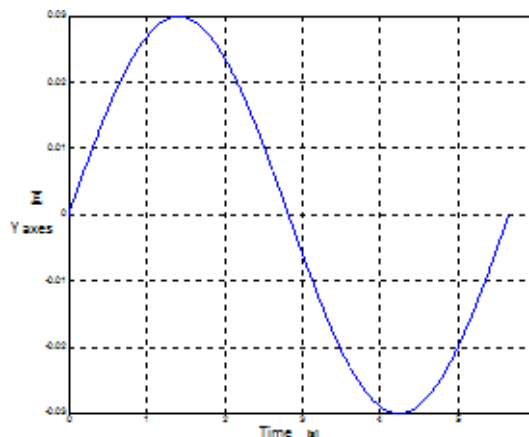


Fig. 4.24: Evolution of the reference position (Y axis)

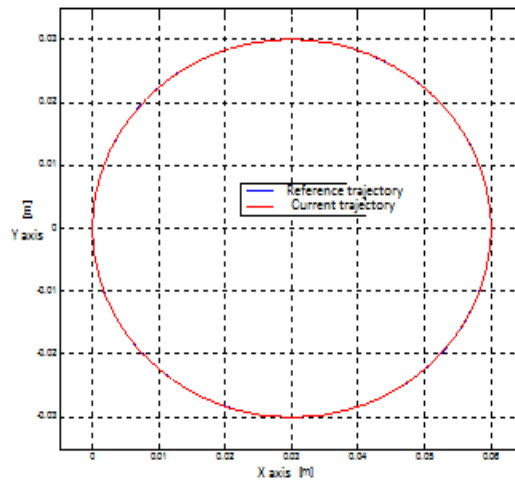


Fig. 4.25: The reference and current tranjectories

In figure 4.26 a-d are presented, at a larger scale, for each of the I-IV quadrants, the two trajectories, namely the reference and current one. It is observed that passing from one quadrant to another, the deviation signal will change (blue line – for reference trajectory and the red line-current trajectory, and how they succed one after the other, at the exterior and interior). From figure 4.26 a-d it can be observed that the X and Y deviations from the two trajectories come in a range of 10 μm .

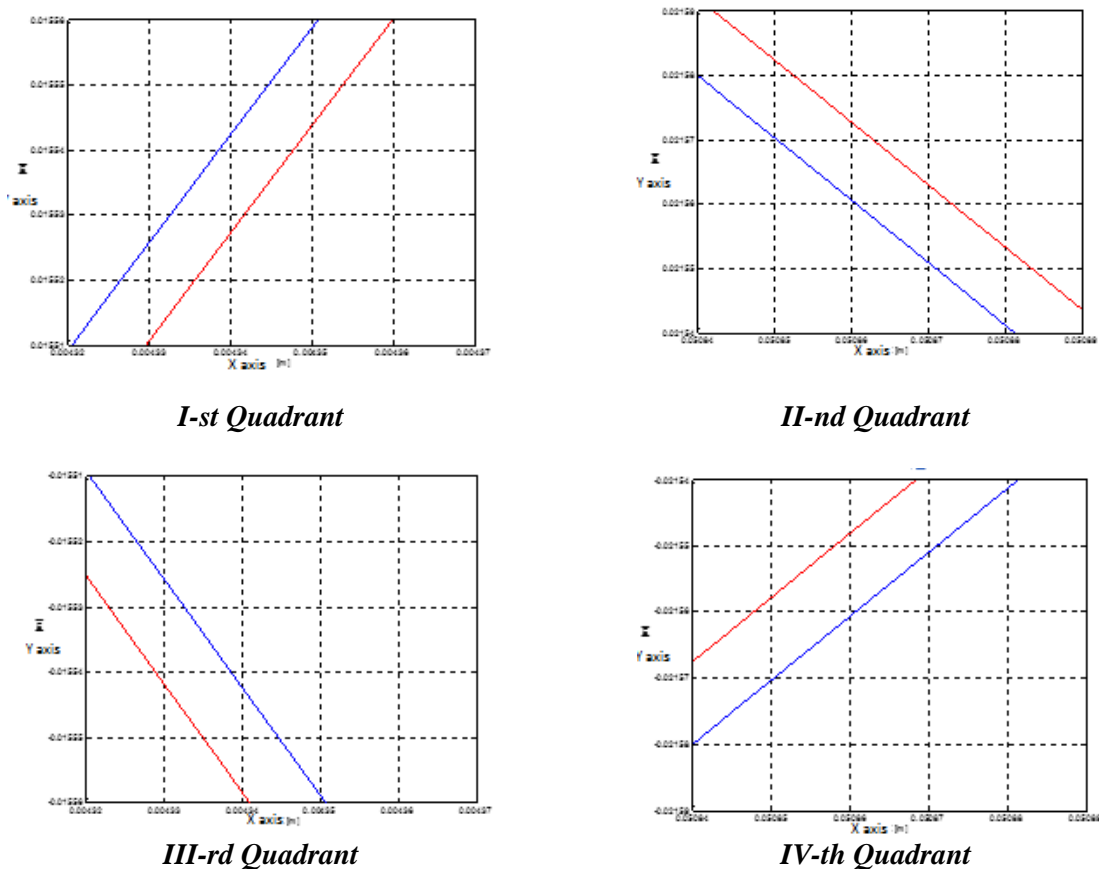


Fig. 4.26: The reference and current trajectories, at larger scale (data presented in the form of quadrants)

In figures 4.27 and 4.28 are presented the evolutions of the follow-up errors for the two axes, X and Y. The maximum value of the follow-up error for the X axis is of 10 μm , while for the axis Y is greater than 27 μm . This fact indicates that the follow-up error does not directly influence

the deviations between the reference and current trajectories. The follow-up errors actually indicate a time delay between the reference and current values of the axes' position.

However, a deviation on the X and Y axis, between the reference and current trajectory, greater than 1 BLU (4 μm), is considered relatively high, although acceptable for the laser cutting procedure. In order to reduce the occurrence rate of these deviations, two strategies were approached:

- increase of derivative of a constant for the position controller (K_d);
- usage of certain proportionality factors, different from those of the two axes.

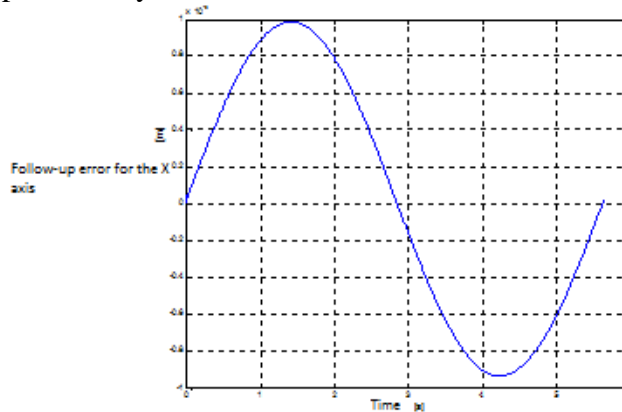


Fig. 4.27: Follow-up error for axis X

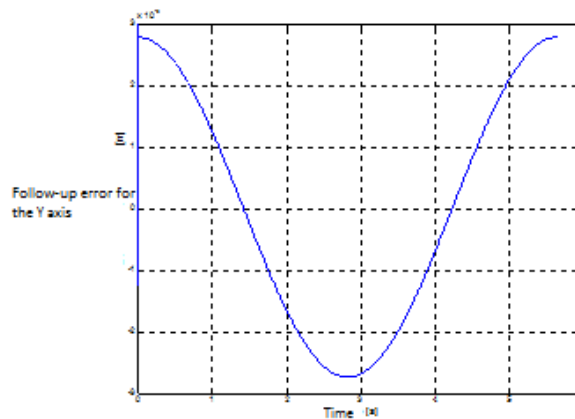


Fig. 4.28: Follow-up error for axis Y

In case of increasing the derivative of a constant for the position controller (K_d), through simulation tests, the behaviour of the system was studied for the $K_d = 1$ value. The main problem that occurred was the increased value registered through the motor inducer of the feeder linkage, which surpasses the admissible maximum value of 132 A.

In figures 4.29 and 4.30 are presented, in comparison to one another, the evolution of the current through motor inducer of the X axis, for both cases, $K_d = 0$ (initial) și $K_d = 1$.

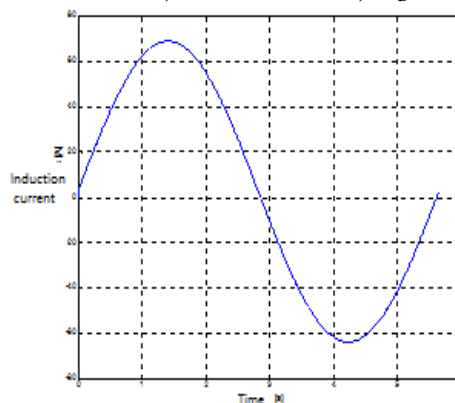


Fig. 4.29: The evolution of the current through motor inducer for X axis ($K_d = 0$)

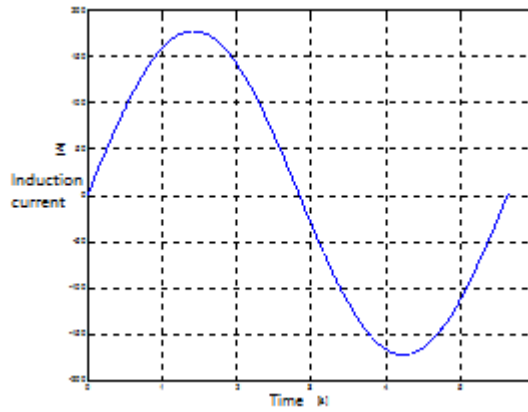


Fig. 4.30: The evolution of the current through motor inducer for X axis ($K_d = 1$)

The second strategy, is based on the fact that the follow-up error for the Y axis is higher than that for axis X, so in order to reduce it, a constant of proportionality for the position controller $K_{py} = 1.5 K_{px}$ was used. For the K_{px} value the initial 2730.7 bit/m range was maintained.

In figure 4.31 is presented the evolution of the follow-up value for the Y axis. It is observed that the maximum value was reduced from over 27 μm to under 22 μm .

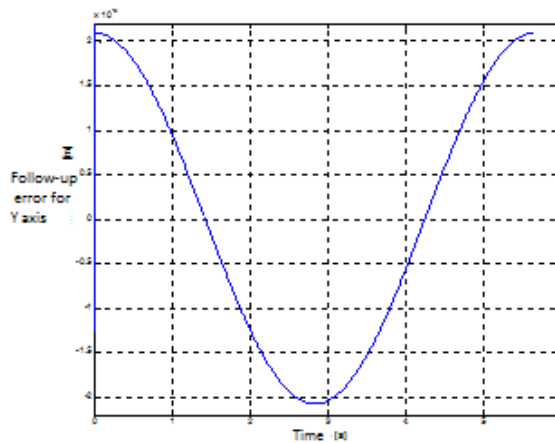


Fig. 4.31: Follow-up error for Y axis ($K_{py} = 1.5 K_{px}$)

In figure 4.32 is presented the evolution of the current through motor induction for the Y axis, which shows that, although the maximum value has increased in comparison to the initial case, the admissible maximum value of 132 A was not surpassed.

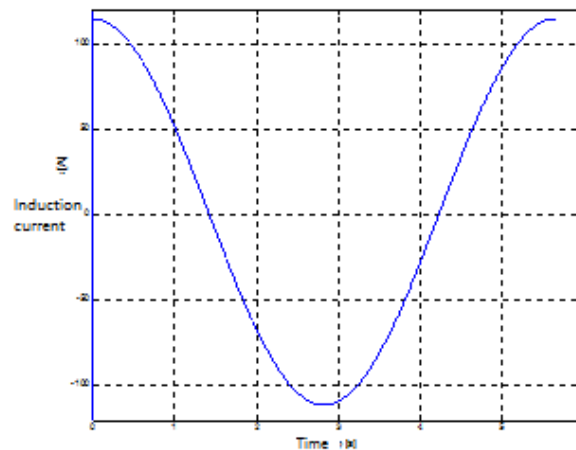


Fig. 4.32: The evolution of the current through motor inducer for the Y axis ($K_{py} = 1.5 K_{px}$)

Still in work, are presented at a larger scale and illustrated for each quadrant I-IV, the two trajectories, the reference and current trajectories, for the new case.

The deviations between the two trajectories of the X and Y axes were reduced, displaying a lower value than that of the grid, with an approximate value of 7 μm . This fact validates the use of certain constants of proportionality adherent to the position controller units, that differ in case of outlined deviation reduction processes.

4.7 The Simulation Study for Generating the 90° Corners

For this purpose, the chart in figure 4.34 was created.

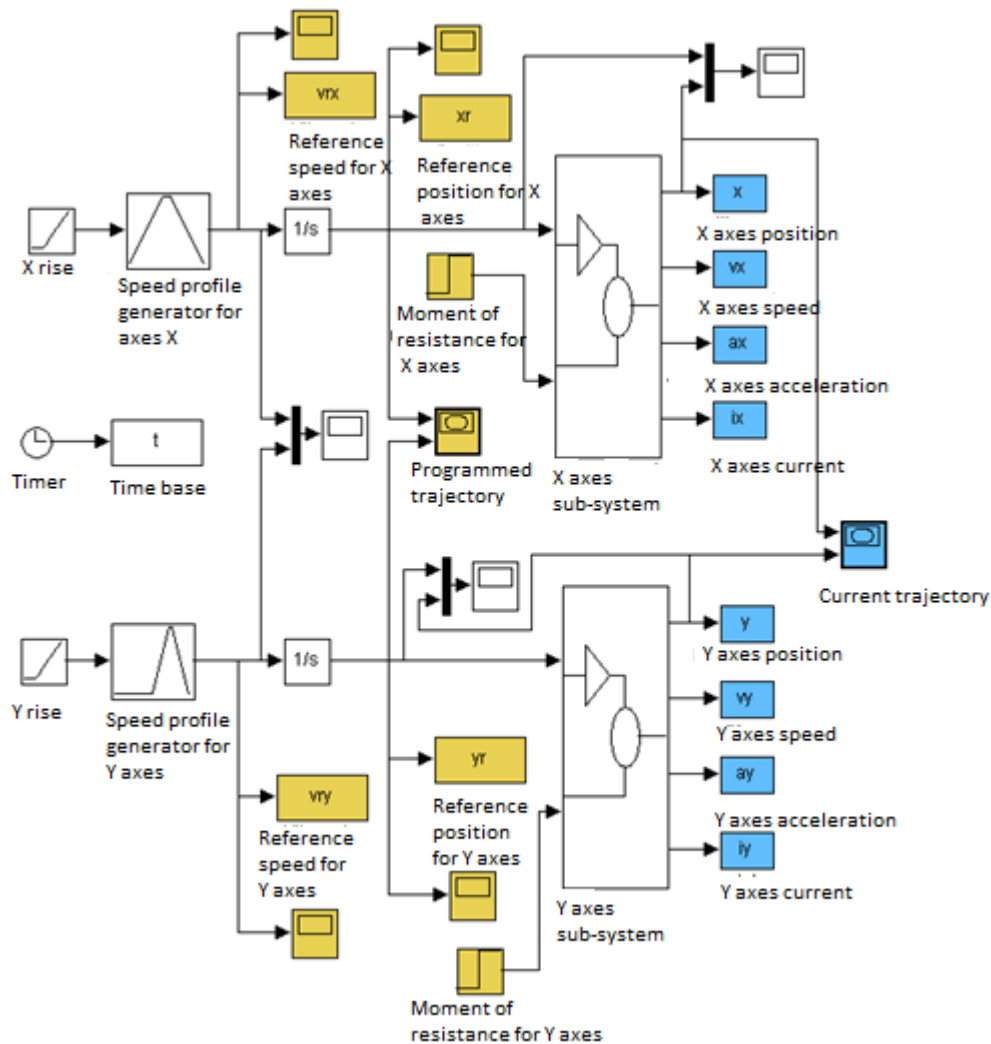


Fig. 4.34: Chart for simulating the generation of 90° corners

The generation of 90° corners presupposes an evolution of the speed variable for the X and Y axes as according to a trapezoidal shape profile, presented in figure 4.35. Therefore, the movement for the Y axis starts immediately after the X axis finishes its' movement.

In the first stage of the simulation, the adjustment constants (of equal value for the X and Y axes) were established at the corresponding values for the outlining mode as:

- the constant of proportionality for the position controller $K_p = 20480 \text{ bit/m}$;
- the derivative of a constant for the position controller $K_d = 0 \text{ bit}\cdot\text{s/m}$;
- feed forward constant for the position controller $K_{ff} = 0 \text{ bit/V}$.

The technical feed rate was set at the maximum value that can be executed by the machine, $F = 15000 \text{ mm/min}$.

Under these conditions, the result of the simulation is presented in figure 4.35.

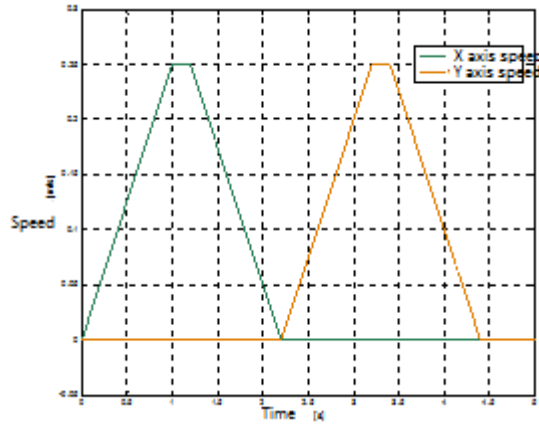


Fig. 4.35: The evolution of speed for axes X and Y

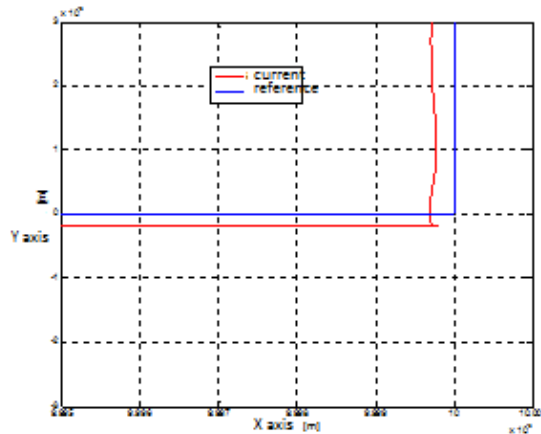


Fig. 4.36: The reference and current trajectories under initial conditions

From figure 4.35 it can be observed that the deviations of the reference and current trajectories are relatively small, with a value under sub 1 μm . From a quality point of view, it can be noted the oscillation behaviour that overlaps the deviation of the reference trajectory. On the X axis, the deviation from the reference trajectory causes an ‘undercut’ while for the Y axis the deviation causes an ‘uppercut’. This is valid for exterior corners. For interior corners the case will be reversed.

Even if the values of the deviations are low, in case the laser beam diameter is an important factor – usually referring to millimetres, these deviations must be reduced.

As a first method to improve the processing procedure, the reduction of oscillations in the corner point is implied by increasing the value of the derivative of a constant for the position controller at a value of $K_d = 10 \text{ bit}\cdot\text{s}/\text{m}$ and keeping the other parameters unchanged. The result of the simulation for this new case is presented in figure 4.37.

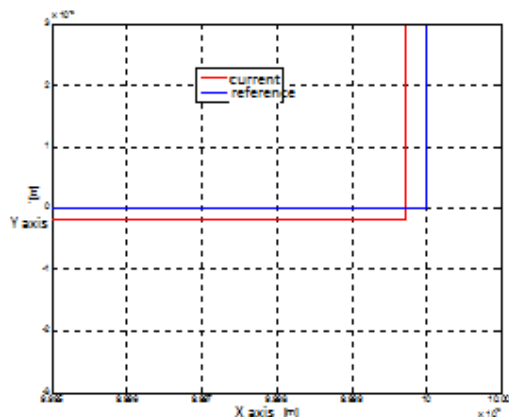


Fig. 4.37: The reference and current trajectories after the change of $K_d = 10 \text{ bit}\cdot\text{s}/\text{m}$

The oscillation was removed but the values of the deviations between the reference and current trajectories for both axes remained unchanged.

In order to reduce these deviations, the feed forward constant was modified for the position controller. In figures 4.38 and 4.39 are presented the results of the simulations for the two values of the feed forward constant, $K_{ff} = 0.1$ bit/V (fig. 4.38) and $K_{ff} = 0.08$ bit/V (fig. 4.39). This approach leads to a reduction in deviations between the reference and current trajectories for the Y axis, the lower value of the deviation was obtained for $K_{ff} = 0.08$ bit/V. However, it should be taken into consideration the nature of the corner, either exterior or interior. In case of an exterior corner a higher reduction for the deviation of the Y axis is recommended, while for an interior corner this reduction can create problems.

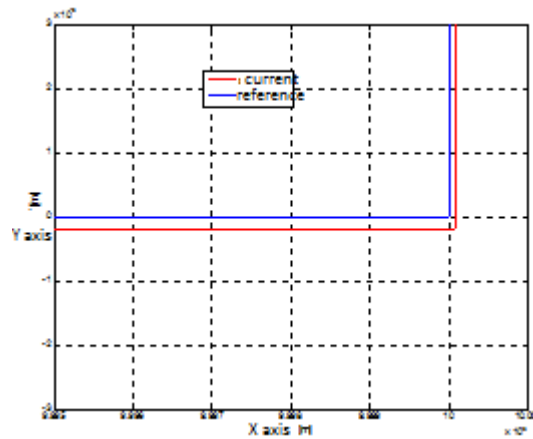


Fig. 4.38: The reference and current trajectories after the adjustment $K_d = 10$ bit·s/m și $K_{ff} = 0.1$ bit/V

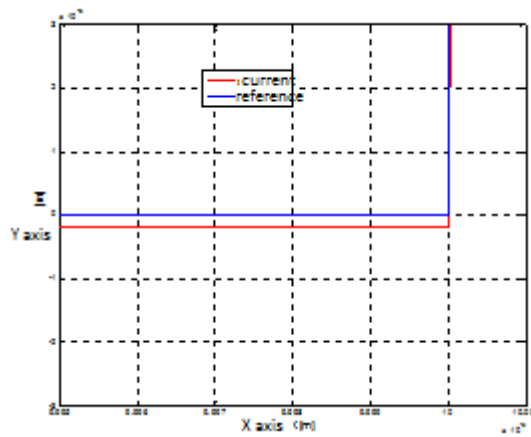


Fig. 4.39: The reference and current trajectories after the adjustment $K_d = 10$ bit·s/m și $K_{ff} = 0.08$ bit/V

4.8. Conclusions

In this chapter a simulation case study was presented, regarding the behaviour of feeder linkages taken from the laser cutting machines with numerical control.

Using the Matlab and Simulink programming package, specific simulation charts were drafted for the main functioning modes:

- fast positioning mode;
- biaxial outlining mode;
- generating the 90° corner mode

The simulations have allowed the testing of different adjustment strategies and conducting useful conclusions for each of the operational mode aforementioned above.

Therefore, for a fast positioning movement it has been constituted that a derivative of a constant higher than zero should be applied to the position controller in order to reduce the oscillations for the position control system.

In case of biaxial outlining mode, the strategy that allowed the obtaining of better results, presupposes the usage of a derivative of a constant for the position controller of zero value, as well as the usage of constants of proportionality of different values from those of axes X and Y.

The generation of the 90° corners has revealed the necessity of using values above zero, for the derivative of a constant and for feed forward constant adherent to the position controller. The first method contributing to the reduction in oscillations and the second for reducing deviations between the reference and current trajectories for to the second motion axes.

Chapter 5

Applied Experimental Research in Relation to the Laser Cutting Machines with Numerical Control

5.1. Equipment Used

The experimental research implied the cutting of certain parts using the laser cutting machine with numerical control brand MAZAK ST-X48 Mk II (figure 5.1) found in property of the S.C. Phoenix & Co SRL company from Sibiu (<http://www.phoenixco.ro>).



Fig. 5.1: Laser cutting machine with numerical control, brand MAZAK ST-X48 Mk II

In table 5.1 are presented some of the main features of the above mentioned machine:

Tabel 5.1

Item No.	Feature	Value/ Remarks
1.	Movement mode for the active elements	X axis -table motion Y axis – motion of the cutting head unit
2.	Maximum sizes of the X x Y semi-finished product	2500 × 1250 mm
3.	Table ground clearance	900 mm
4.	Power of the laser oscillator	1.5 KW

5.	Maximum capacity for loading the table	300 Kgf
6.	Maximum length of the run for the X axis	2685 mm
7.	Maximum length of the run for the Y axis	1270 mm
8.	Maximum length of the run for the Z axis	100 mm
9.	Feed rate maximum speed for the X and Y axes	24 m/min
10.	Feed rate maximum speed for the Z axes	25 m/min
11.	Technical advance maximum speed	15 m/min
12.	Type of actuation	Servo motors $\alpha 6/3000$ GE Fanuc
13.	Transmission of the X, Y axes	Ballscrew
14.	Transmission of the Z axis	Belts
15.	Position precision for the X, Y axes	$\pm 0.01/500$ mm
16.	Position precision for the Z axis	$\pm 0.01/100$ mm

In order to determine the precise dimensions of the processed parts, a set of measurement values were established using a coordinate measurement machine MMC.

Measurements were performed at the S.C. Sirfit SRL company, Sibiu subsidiary of the Italian company Fonderie Officine Meccaniche Tacconi (<http://www.fomtacconi.it>), on a DEA Global Silver Performance coordinate measurement equipment.

5.2. Processed Parts

During the experimental research, 3 types of parts had been processed as presented in figures 5.3-5.5. In these pictures the quotas that have been measured using the coordinate measuring machine are also indicated. Each of these quotas have been marked with a hexagon symbol filled in with the serial number of the quota.

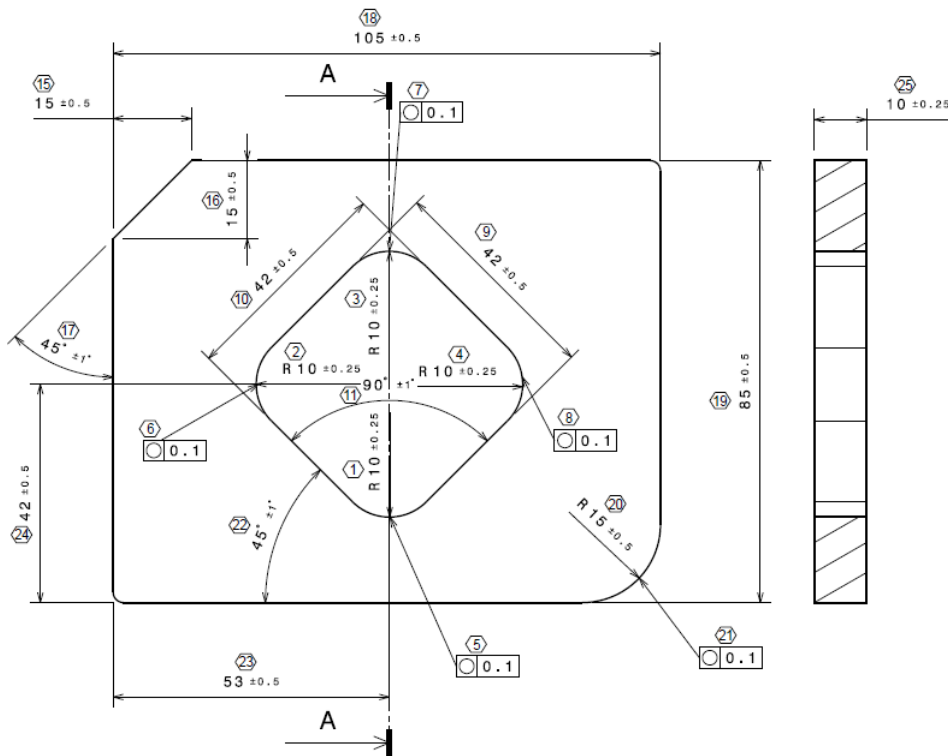


Fig. 5.3: Test part No.1

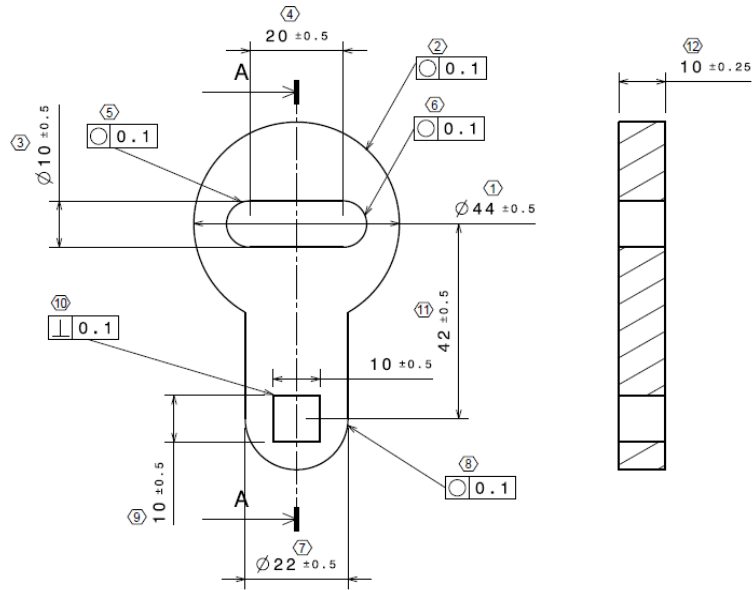


Fig. 5.4: Test part No. 2

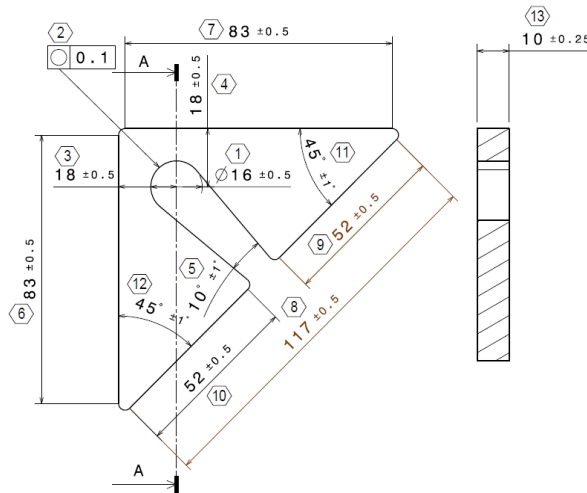


Fig. 5.5: Test part No.3

Therefore, a number of 24 quotas were verified for test part No.1, 11 quotas for test part no.2 and 12 quotas for test part no.3.

The shapes of the parts were especially chosen in order to test:

- the precision of the forward working motions for linear and circular trajectories;
- the precision of generating corners (compression).

In figure 5.7 are presented some of the processed parts.



Fig. 5.7: Processed parts

5.4 Experimental Research on the Outline Cutting Precision

The first stage of the experimental research, meaning the adjustment parameters of the numerical control equipment were set for both axes at the values presented below:

- the constant of proportionality for the position controller $K_{px} = K_{py} = 2730.7$ bit/m;
- the derivative of a constant for the position controller $K_{dx} = K_{dy} = 0$ bit·s/m;
- the feed-forward constant of the position controller $K_{ffx} = K_{ffy} = 0$.

These values correspond to those resulted from theoretical calculus and are identical to those used in the simulation tests shown in paragraph 4.6.5. of the present paper.

The feed rate was established at 2000 mm/min and the semi-finished product has a 10 mm thickness.

Initially, a piece of test part no.1 was cut and the control quotas 15 and 16 were measured as according to figure 5.8:

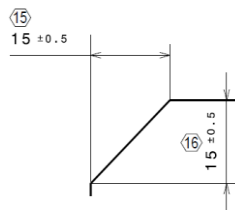


Fig. 5.8: Quota 15 and 16

The measured quotas were as follows:

- quota 15: 15.2040 mm;
- quota 16: 14.9224 mm.

The next measurement was done for quota 19 (fig. 5.9) which represents a linear dimension that ends with a circular arc of 15 mm radius. The measured value was:

- Quota 19: 84.8594 mm.

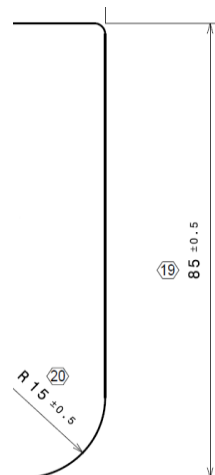


Fig. 5.9: Quota 19

Based on the results of these measurements, especially those referring to quota 15 and 16, as well as on the theoretical research, it was concluded that: in order to increase the precision value of the outline it is recommended that the proportionality factor of the position controller to be increased for axis Y. This approach is justified by the value of quota 16 which is lower than the nominal value of 15mm, fact that indicates that the proportionality factor for the Y axis is too low.

Thus, the adjustment constants' value was modified according to those mentioned below:

For axis X

- the constant of proportionality for the position controller $K_{px} = 2730.7$ bit/m;
- the derivative of a constant for the position controller $K_{dx} = 0$ bit·s/m;
- feed-forward constant for the position controller $K_{ffx} = 0$.

For axis Y (two possibilities)

- the constant of proportionality for the position controller $K_{py} = 3726.84$ bit/m, $K_{py} = 4096.05$ bit/m;
- the derivative constant of the position controller $K_{dy} = 0$ bit·s/m;
- the feed-forward constant for the position controller $K_{ffy} = 0$.

The constant of proportionality K_{py} was initially increased to a value equal to $1.2 \times K_{px}$ and afterwards to $1.5 \times K_{px}$.

In order to validate the proposed approachment, two pieces from test part no.1 were cut using the modified adjustment parameters and the same feed rate value of 2000 mm/min.

The results for quota 15,16 and 19, before and after the parameters have been modified, are presented in table 5.4.

Table 5.4

Value of the adjustment parameters	Quota 15 (nominal value of 15 mm)	Quota 16 (nominal value of 15 mm)	Quota 19 (nominal value of 85 mm)
$K_{px} = K_{py} = 2730.7$ bit/m $K_{dx} = K_{dy} = 0$ bit·s/m $K_{ffx} = K_{ffy} = 0$ $F = 2000$ mm/min	15.2040	14.9224	84.8594
$K_{px} = 2730.7$ bit/m $K_{py} = 3726.84$ bit/m $K_{dx} = K_{dy} = 0$ bit·s/m $K_{ffx} = K_{ffy} = 0$ $F = 2000$ mm/min	15.1706	14.9795	84.9024
$K_{px} = 2730.7$ bit/m $K_{py} = 4096.05$ bit/m $K_{dx} = K_{dy} = 0$ bit·s/m $K_{ffx} = K_{ffy} = 0$ $F = 2000$ mm/min	15.1385	14.9649	84.9175

According to the results presented in table 5.4, the increase in value of the constant of proportionality for axis Y reduces the value of the obtained deviation as compared to the nominal value of the quota. Furthermore, it is noted that the resulted improvement, by increasing the K_{py} from $1.2 \times K_{px}$ to $1.5 \times K_{px}$, is practically insignificant for this type of process.

In order to confirm the efficiency of the proposed method, the behaviour of the circular outline cutting operation must be studied. Therefore, three pieces of test part no.2 were processed under the same conditions as test part no.1, again using a metal sheet of 10 mm thickness. With the help of the coordinate measuring machine, the $\varnothing 44$ mm diameter circular outline was processed.

The coordinate measuring equipment can display the maximum circular deviation value, but this value is insignificant in this case, for it indicates a maximum local value that might have intervene accidentally.

For a better analysis of the circular outline cutting precision, the following method was used and the stages are presented below:

- ✓ the scanned points from the circular outline were saved with the help of the MMC in a graphics file with the igs extension (fig.5.10);

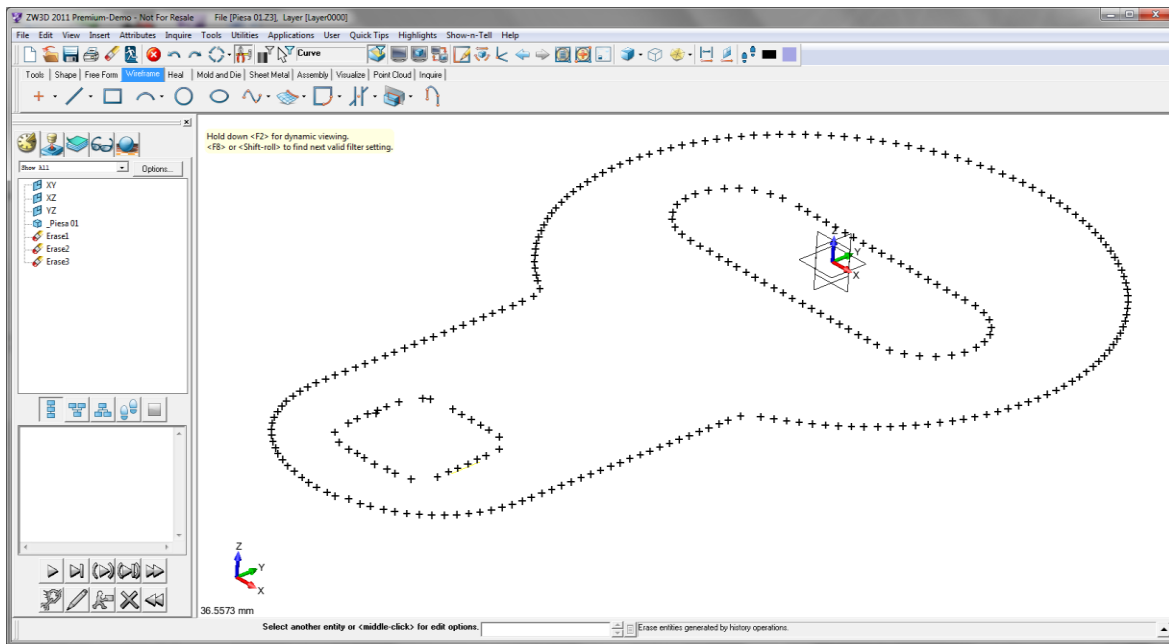


Fig. 5.10: The igs extension file with the points scanned with the help of MMC

- ✓ with the help of a specialised programme (ZW3D) the circular outline was redrafted by connecting the obtained points with the spline curves, using the "point clouds" processing technology (fig. 5.11);
- ✓ with the help of another programme (SputCAM, computer assisted processing programme), an increased number of points as compared to the MMC scanning, was extracted from the redrafted circular outline and their coordinates were saved;
- ✓ based on these coordinates, the circular outlines were then compared using the Matlab programme.

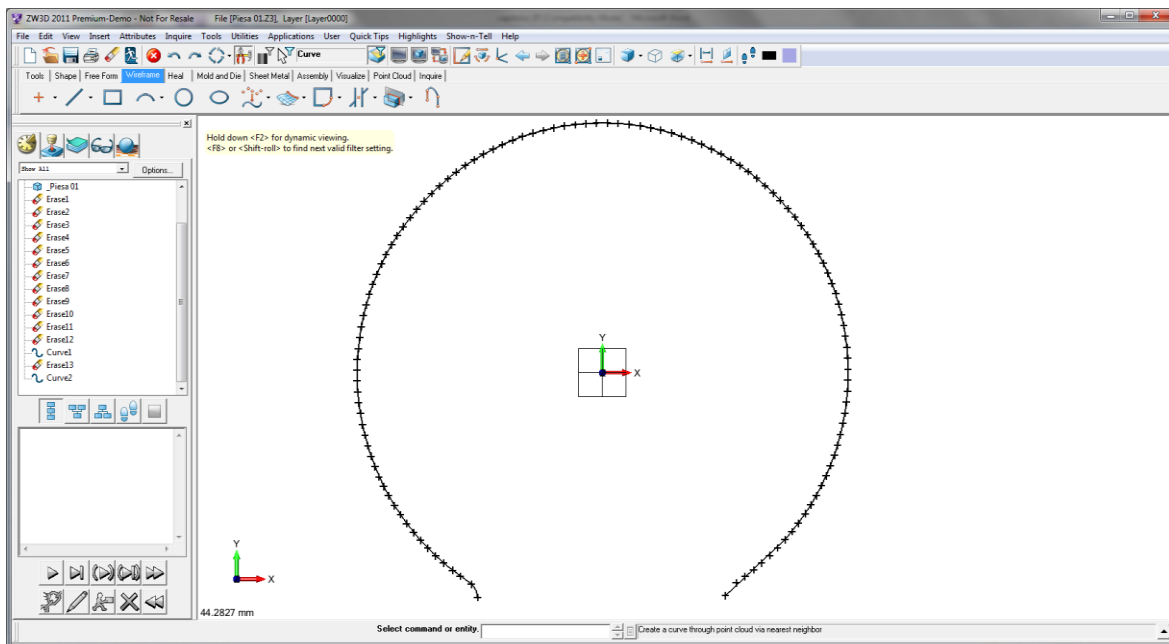


Fig. 5.11: The circular outline redrafted by using the point clouds processing method

In table 5.5 are presented the coordinates of the points taken from the circular outline, obtained from all three cases and the coordinates of a standard circle of $\varnothing 44$ mm.

Table 5.5 (excerpt)

Standard circle		Circular outline 1 $K_{px} = K_{py} = 2730.7$ bit/m $K_{dx} = K_{dy} = 0$ bit·s/m $K_{ffx} = K_{ffy} = 0$ $F = 2000$ mm/min		Circular outline 2 $K_{px} = 2730.7$ bit/m $K_{py} = 3726.84$ bit/m $K_{dx} = K_{dy} = 0$ bit·s/m $K_{ffx} = K_{ffy} = 0$ $F = 2000$ mm/min		Circular outline 3 $K_{px} = 2730.7$ bit/m $K_{py} = 4096.05$ bit/m $K_{dx} = K_{dy} = 0$ bit·s/m $K_{ffx} = K_{ffy} = 0$ $F = 2000$ mm/min	
x_e	y_e	x_{c1}	y_{c1}	x_{c2}	y_{c2}	x_{c3}	y_{c3}
22.	0.54	11.116	-19.385	11.21	-19.254	11.18	-19.336
21.947	1.619	11.414	-18.993	11.564	-18.821	11.503	-18.914
21.841	2.694	11.752	-18.634	11.954	-18.42	11.865	-18.526
21.683	3.762	12.126	-18.312	12.378	-18.055	12.263	-18.175
21.472	4.822	12.329	-18.172	12.606	-17.892	12.479	-18.02
21.209	5.869	12.737	-17.89	13.02	-17.596	13.014	-17.635
20.896	6.903	12.938	-17.751	13.213	-17.457	13.21	-17.494
20.532	7.92	13.135	-17.608	13.402	-17.312	13.4	-17.344
				13.605	-17.156	13.778	-17.041

In figure 5.12 is presented the graphic obtained in the Matlab programme, by using the point coordinates taken from table 5.5, and figures 5.13 -5.16 and the details of this representation for each of the 4 quadrants. It can be observed that the experimental results confirm the proposed strategy, meaning using different amplification factors for the two axes.

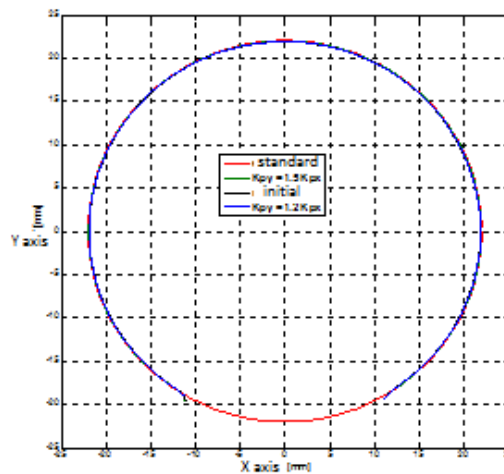


Fig. 5.12: The graphical representation of the experimental results for the exterior circle with $\varnothing 44$ mm

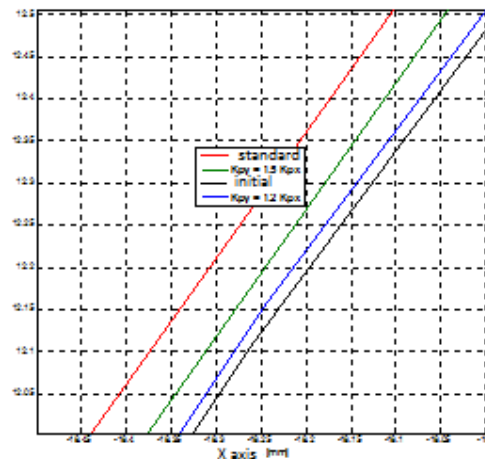


Fig. 5.13: The graphical representation of the experimental results for the exterior circle with $\varnothing 44$ mm (detail, 1-st quadrant)

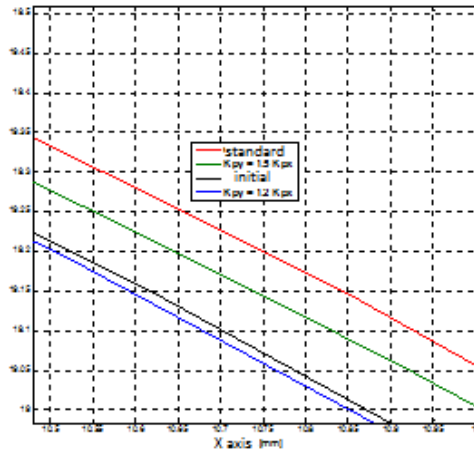


Fig. 5.14: The graphical representation of the experimental results for the exterior circle with Ø44 mm (detail, II-nd quadrant)

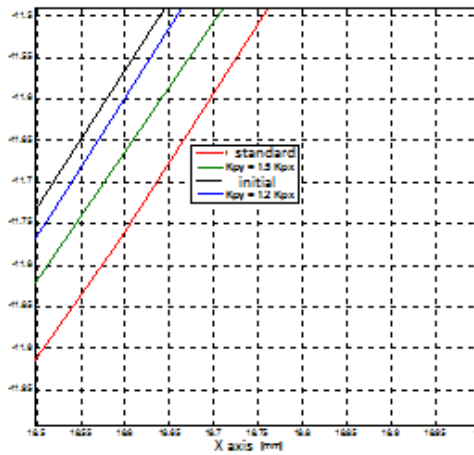


Fig. 5.15: The graphical representation of the experimental research for the exterior circle with Ø44 mm (detail, III-rd quadrant)

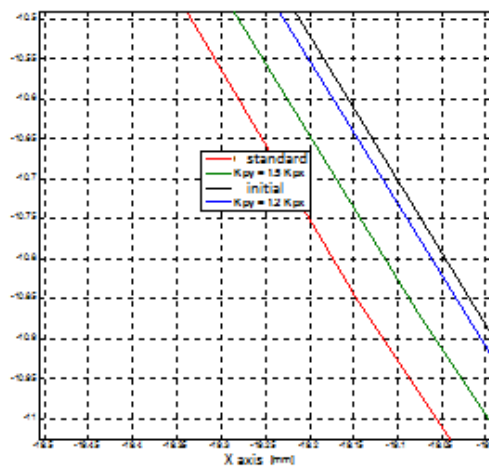


Fig. 5.15: The graphical representation of the experimental results for the exterior circle with Ø44 mm (detail, III-rd quadrant)

5.5 Experimental Research on the Cutting Precision for the 90° Corners

The testing of the 90° corner cutting precision was undertaken by cutting four pieces from test part no.2, semi-finished product of 2 mm thickness with a feed rate of $F = 15000$ mm/min.

In order to test the strategy set by means of the theoretical research, presented in paragraph 4.7, the adjustment parameters were set at:

1. $K_p = 20480$ bit/m, $K_d = 0$ bit·s/m, $K_{ff} = 0$ bit/V;
2. $K_p = 20480$ bit/m, $K_d = 10$ bit·s/m, $K_{ff} = 0$ bit/V;
3. $K_p = 20480$ bit/m, $K_d = 10$ bit·s/m, $K_{ff} = 0.1$ bit/V;
4. $K_p = 20480$ bit/m, $K_d = 0$ bit·s/m, $K_{ff} = 0.08$ bit/V;

One of the corners from the interior outline was measured (fig. 5.18). For this procedure a profilometer was used.

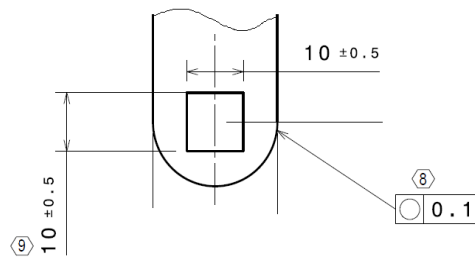


Fig. 5.18: The interior outline with 90° corner

In figures 5.19-5.22 are presented the results of the experimental determination. The measurement was done at the center of an imaginary circle, inscribed in the corner with $\varnothing 4$ mm.

It can be noticed that the measured values confirm, from a quality point of view, the results obtained by means of simulation and presented in paragraph 4.7.

The dimensional precision of the processed outline registers an increase, starting with part no.1 and ends with part no.4, and thus validating the proposed strategy.

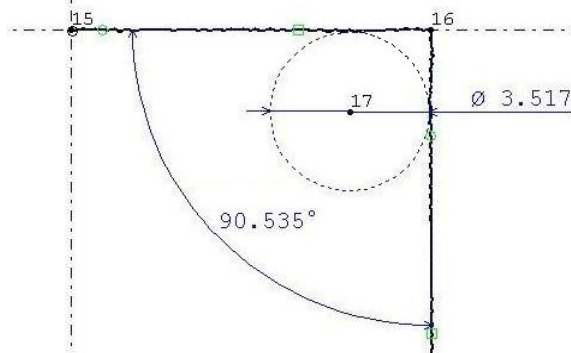


Fig. 5.19: 90° corner ($K_p = 20480$ bit/m, $K_d = 0$ bit·s/m, $K_{ff} = 0$ bit/V)

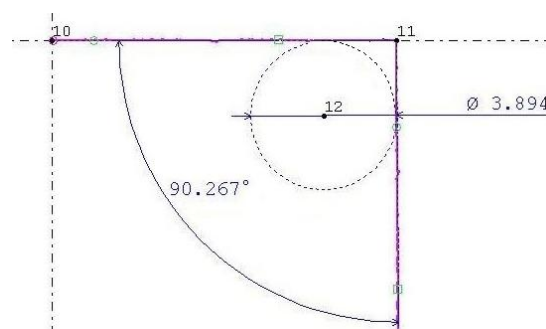


Fig. 5.20: 90° corner ($K_p = 20480$ bit/m, $K_d = 10$ bit·s/m, $K_{ff} = 0$ bit/V)

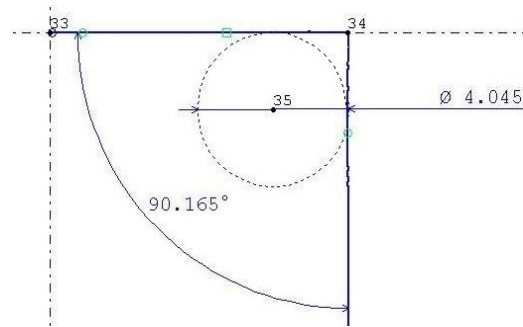


Fig. 5.21: 90° corner ($K_p = 20480 \text{ bit/m}$, $K_d = 10 \text{ bit}\cdot\text{s/m}$, $K_{ff} = 0.1 \text{ bit/V}$)

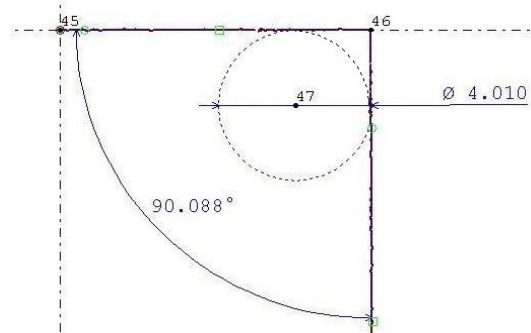


Fig. 5.22: 90° corner ($K_p = 20480 \text{ bit/m}$, $K_d = 10 \text{ bit}\cdot\text{s/m}$, $K_{ff} = 0.08 \text{ bit/V}$)

5.6. Applied Research Regarding the Carving Process of Semi-Finished Products

5.1.3 Method of calculus for the degree of usage for the material, based on image processing operations

The presented method implies the usage of the Matlab software package and of the Image Processing toolbox (Matlab appendix). Even for the commercial version of the programme, the necessary applied software resources for this method do not surpass 1800 EURO.

According to the assisted computer image processing theory, an image is divided in N rows and M columns. The junction of one row with another column is called pixel, representing the base element of a computer image and $a[m,n]$ representing the associated value of a coordinate point $[m,n]$.

The image file that will be processed represents the carving plan. This plan is supplied to the user under the form of a black/white image saved according to the following formats:

- ***dxf*** (Drawing Exchange Format);
- ***dwg*** (Drawing);
- ***bmp*** (Bitmap),
- ***tiff*** (Tagged Image File Format), the short version of ***tif*** is used;
- ***jpeg*** (Joint Photographic Experts Group) the short version of ***tif*** is used.

The ***dxf*** and ***dwg*** format are specific formats used with computer assisted design projects that operate with 2D drawings, and the ***bmp***, ***tif*** and ***jpg*** format are especially design for image processing programmes.

The conversion from/in any of the above mentioned formats can easily be done and there are many other free programmes that can do this operation.

In order to apply the proposed method, the most recommended formats are ***tif*** and ***jpeg***.

The application method of calculating the material's degree of usage will be described starting with the carving plan described in figure 5.25.

The semi-finished product from figure 5.25 has a size of 600 × 400 mm and the carving plan sets the cutting frame to process 7 pieces.

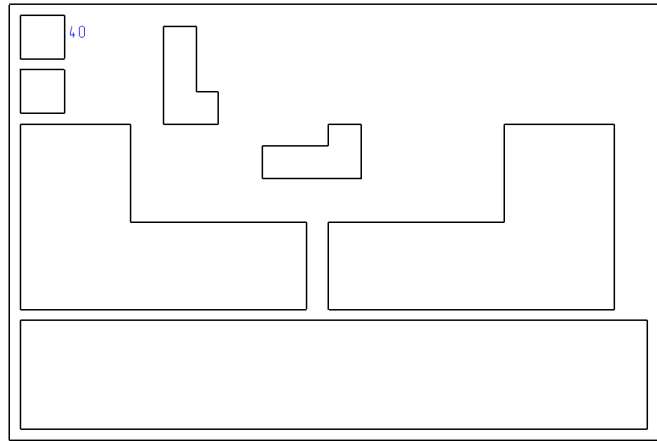


Fig. 5.25: Carving plan used to illustrate the proposed method

As stated above, the carving plan is supplied under the format of a graphics file, most of the time at an arbitrary scale (which is influenced by the necessity to print the file on a A4 format or smaller). It must be taken into consideration that the image processing programmes operate with pixel type units while the real parts or the semi-finished products are stated in millimeters.

As a first stage, a Matlab programme was created to allow the calculus of the E factor scale, defined as:

$$E = \frac{e}{c} \left[\frac{\text{pixels}}{\text{mm}} \right] \quad (5.1)$$

where

E is scale factor [pixels/mm];

e –pixel value of the standard distance, interactively measured;

c – the mm value of the standard distance (drawing rate).

The pixel value of the standard distance is calculated using the relation:

$$e = \sqrt{(r_f - r_i)^2 + (c_f - c_i)^2} \quad [\text{pixels}] \quad (5.2)$$

where:

$r_{i,f}$ is the initial and respectively the final value of the lines on which the selected pixels are present

$c_{i,f}$ –the initial and respectively final value of the columns on which the selected pixels are present

After calculating the scale factor, any physical distance expressed in mm from the carving plan, can be determined according to the formula below:

$$d = \frac{d_{mas} \left[\frac{\text{pixels}}{\text{mm}} \right]}{E} \quad [\text{mm}] \quad (5.3)$$

where:

d is the value of the physical distance, respectively of the real rate of the part taken from the carving plan [mm]

d_{mas} –the value of the pixel distance interactively determined from the carving plan

The programme, created in Matlab and presented in the appendixes, allows the interactive graphical selection of the two points that limit the standard distances, rated in the figure representing the carving plan, and then it automatically calculates the E scale factor, defined by the (5.1) relation. Certain operator defined functions were set to allow the graphic control of the

image, the length and display of the standard distance. Therefore, the shape, size and colour of the markers can be controlled, data which limit the standard distance as well as the position, colour and size of the displayed text. In the next stage, the programme saves the calculated value as a ASCII type text file.

For the carving plan presented in figure 5.25, the mm value of the standard distance, rated on the drawing, is of 40 mm. In figure 5.26 is presented the part of the carving plan after the standard distance had been selected.

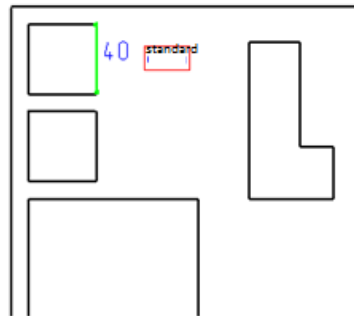


Fig. 5.26: The selection of the standard distance, rated on the drawing

The calculated scale factor has the $E = 1.45$ pixels /mm value.

In order to calculate the material's degree of usage it is necessary to measure the surface of the area, of the semi finished product and of the parts, by interactively selecting them from the carving plan.

As such a Matlab programming medium (presented in the appendix) was created to allow the interactive selection of the points adherent to a closed outline and the calculus of a limited area in order to repeat this action whenever it is necessary.

For semi finished products, the programme comes in two versions, with and without holes.

In general, the running of the programme (for the "no hole" version) requires the fulfilment of the following stages:

- Data entry of the following information by the operator from the keyboard:
 - the name and graphic file extension contained by the carving plan;
 - the E scale factor value, in pixels/mm;
 - the total number of parts from the carving plan;
 - the total number of holes from the carving plan.
- The interactive selection of the 4 corners adherent to the semi finished product of the metal sheet and the calculus of its' surface (the programme allows the calculus of the area surface of the semi finished product even if the product is not of rectangular shape);
- The interactive selection of the parts' outline and the calculus of the total surface area occupied by it. In this stage, a "for" cycle was introduced in the programme and is will be executed a number of times, equal to the number of parts contained by the carving plan.;
- The interactive selection of the hole's outline and the calculus of the total area surface occupied by it. In this stage, a "for" cycle was introduced in the programme and a number of times equal to the number of parts from the carving plan will be executed;
- Calculating the percentage calculus of the degree of usage, adherent to the semi finished product, using the formula:

$$g = \frac{AP}{S} \times 100 \text{ [%]} \quad (5.4)$$

where:

g is the degree of usage of the material[%];

S –the surface area of the semi finished product [mm²];

AP –the useful surface area occupied by the parts [mm²].

For the occupied useful surface area by the parts, we use the relation:

$$AP = P - G \text{ [mm}^2\text{]} \quad (5.5)$$

where:

P is surface area of the parts [mm²];

G –the surface area of the holes (orifice) [mm²].

In figure 5.27 is presented a screenshot taken while the programme was running. The shot was taken after the interactive selection of the semi finished product was made for eight out of nine parts. The dotted lines can be observed indicating that at the time of the shot, the outline of the second part was interactively selected. It can also be noted that for circular arcs, the user must approximate these outline frames by using line segments, by repeatedly clicking, meaning selecting, a sufficient number of points to assure the calculus of a high level of precision. It can also be considered that the errors issued by these approximations do not significantly influence the accuracy of the result.

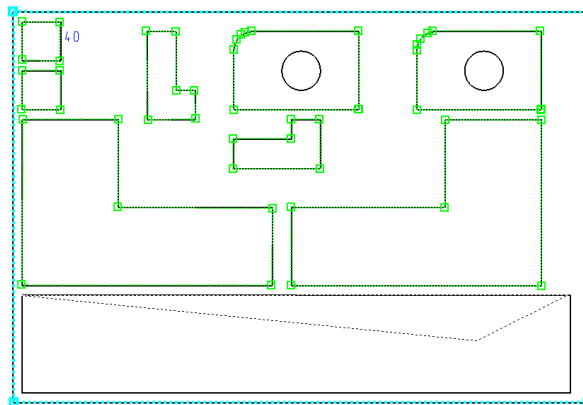


Fig. 5.27: The interactive selection of the points presented on the outline of the semi finished products and parts

In figure 5.28 is presented, at a large scale, a detail that helps approximate the circular outlines (the part's exterior outline is marked in green and the outline of the hole in yellow – the material will be carved out from the part).

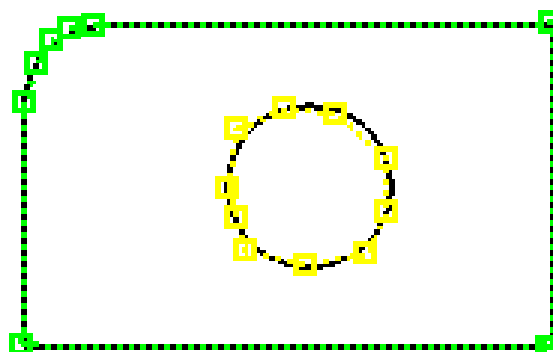


Fig. 5.28: Circular outlines

The programme also saves the results as text files, for possible later use.

The material's degree of usage, calculated for the carving plan in figure 5.5 was of $g = 60.24\%$.

Chapter 6

Final Conclusions and Contributions

6.1. Final Conclusions

The theoretical and experimental research undertaken during the drafting of the present PhD thesis has as main study object the investigation of certain technological improvement methods for laser cutting machines with numerical control, especially by increasing the dimensional precision of the processed parts.

The main concern was to find theoretical and practical solutions that present a high degree of applicability and that can easily be implemented for small and medium size enterprises/companies that use such machinery.

In the first chapter of the paper, the fundamental notions of the theory for mathematical systems and those notions that help base the current theoretical research were presented. The linkages of the laser cutting systems with numerical control were modelled as automated adjustment systems, and described as transfer functions.

In the second chapter of the paper, a critical analysis of the current status was performed, regarding the laser cutting machines with numerical control. The main directions - mechanical structural point of view, transmissions, modes and control units were synthesised and the basic identification methods were noted regarding the improvements of their technological performances.

The important adjustment strategy was analysed at the level of motion control system taken from the structure of the feeder linkages of these machines, highlighting the adherent advantages and disadvantages.

At the end of the second chapter, certain preliminary conclusions were drafted that established the main objectives of the theoretical and practical research.

In chapter three of the present paper, the mathematical model of the feeder linkages taken from the structure of the laser cutting machine with numerical control was presented. As stated above, the model has its basis on the continuous variables of the transfer functions. It is all based on a relatively known version of the mathematical model for the direct current motor, assimilated as an automated revolution adjustment system and later on specific position adjustment elements were added. Based on the preliminary theoretical research, a proposed structure of the position controller was presented, that reproduces as trustworthy as possible the control effects encountered with the industrial numerical control. It was thus researched if the adjustment parameters taken from the proposed structure model are to be encountered more often with the laser cutting machines with numerical control. Furthermore, it was created and integrated within the structure of the generated model of the feeder linkage a calculus model for the technical moments and forces of resistance.

The fourth chapter was entirely dedicated to simulation studies. It was decided that the software instruments for this research to consist from Matlab and Simulink programmes, due to performance, increased level of usage and of the acceptable costs. The main feeder linkages were identified for laser cutting machines with numerical control (fast positioning operation, biaxial outlining operation and the generation of 90° corners); and simulation studies were conducted for each of these operational modes.

For each of the actions described above it was necessary to create a specific simulation diagram. Each of these diagrams is based on the mathematical model developed in the third chapter, but comprising different components to generate the kinematic parameters (position, speed, acceleration) for each operational mode.

The simulations allowed the proposal of certain adjustment strategies that can improve the dynamic behaviour and the kinematic precision of the control systems taken from the linkage structure and implicitly the improvement of dimensional precision for the processed parts.

The fifth chapter is dedicated to experimental and applied research. Therefore, in the first part of the chapter the experimental validation processes for the proposed adjustment theoretical strategies were presented. And thus, a multitude of parts have been processed from semi finished products with different thickness values, by successively modifying the adjustment parameters according to the recommendations resulted from the theoretical research. The parts were later measured and their dimensional precision confirmed and validated the theoretical results and recommendations.

Also within the content of the present chapter, a method that allows the calculus of the material's degree of usage within a carving plan was developed, based on image processing, a method with multiple practical applications.

In the end, based on the conducted research and on the theoretical and applicative results obtained, the following conclusions can be drafted:

From a theoretical point of view

- the feeder linkages, considered as automated motion control systems, present an increased improvement potential for the laser cutting machine processing with numerical control, especially by increasing the dimensional precision of the processed parts
- the mathematical modelling of these systems can be done with the help of the transfer functions, due to the easy operation that describes the behaviour of an automated system, as well as due to the existence of numerous software packages that operate with these mathematical tools
- the modelling must take into consideration the real industrial equipments. The variable parameters of the model must be found within the operator panel of the numerical control equipment, taken from the structure of the laser cutting machines.
- The adjustment of the position controller from the motion control automotive system, by modifying the adjustment constants represents the main method through which the feeder linkage behaviour can be influenced.

From an experimental point of view

- the adjustment of the controllers, mentioned above as a form of strategy, was validated from an experimental point of view as representing the main means through which the dimensional precision of processed parts can be improved
- even if the dimensional deviation highlighted by the simulation studies does not always correspond, from a quality point of view to the experimental one, the evolutions and behaviours of these deviations are similar in quality.
- The usage of modern measuring means (like coordinate measuring equipment) does not always directly solve the problems corresponding to the dimensional estimation of the processed parts. There are cases (like circular outlining cutting) when the supplied data, issued by this type of measuring equipment, must be subject to subsequent analysis and processing processes.

6.2 Personal Contributions

During the drafting process of the present paper, the author brought about his personal contribution. Some of these contributions were presented and published in works presented at international conferences, others are still in the process of publication.

From the theoretical point of view, the following can be mentioned:

- ☑ the drafting of the current critical analysis within the field of laser cutting machines with numerical control technical processing, based on the summary of the literature;
- ☑ the development of a mathematical model for feeder linkages taken from the structure of a laser cutting machine with numerical control, by integrating an existent model of the direct current servo motor within an industrial position controller model and by calculating the technological moment and forces of resistance;
- ☑ the transposition of the model within functional unit blocks for the simulation study with the help of the Matlab and Simulink software;
- ☑ the creation of the Matlab and Simulink package for the simulation sub-systems, necessary for generating kinematic parameters (position, speed, acceleration) adherent to fast motion, circular interpolation and successive movement on two axes;
- ☑ the integration of these sub-systems in simulation diagrams for the feeder linkage behavioural study of the fast positioning mode, biaxial outlining and the generation of 90° corners);
- ☑ the drafting of certain strategies and recommendations to adjust different position controllers to different functional modes.

From an experimental research point of view, the following can be mentioned:

- ☑ the setting up of an experimental processing programme for a set of parts, under different functioning conditions of the motion control systems and to evaluate their dimensional precision;
- ☑ the experimental validation of adjustment strategies established during the theoretical researches by means of modelling and simulation;
- ☑ elaborating certain methods used in subsequent processing of the geometrical data supplied by the coordinate measurement machines; with the main objective of estimating the precision with which the circular outlines are generated;
- ☑ setting up certain programmes in Matlab and Simulink to interactively analyse images and the calculus of some geometrical elements of distance and disk type, having as starting point the image graphics file generated for the carving plan.

6.3. Possible directions taken by the present research paper

As the present paper was drafted taking into consideration the efforts made by previous members of the research center from the ‘‘Lucian Blaga’’ University from Sibiu, Faculty of Engineering, it can be stated that this work can later on be continued within the following research fields:

- study of the machine, possibilities of improving the laser cutting machine with numerical control technology;
- setting up certain mathematical models for the feeder linkages, using the permanent magnet synchronous motor as execution element
- Setting up a technological databases of the system-expert type, applied at the laser cutting processing level of operation

Bibliography (selective)

- Ahn, D.G., Kim, M.S., Lee, S.H., Park, H., Yoo, Y.T., *Influence of process parameters on the kerfwidth for the case of laser cutting of CSP 1N sheet using high power CW Nd:YAG laser*, Journal of the Korean Society of Precision Engineering 22(7) pp.19–26, 2005
- Aichele, G., Nickenig, L., *Tăierea cu fascicul laser - principiul laserului și indicații de deservire privind laserele uzuale*, Sudura nr. 1, an XV, 2005
- Al-Sulaiman, F., Yilbas, B., Ahsan, M., *CO2 laser cutting of a carbon/carbon multi-lamelled plain-weave structure*, Journal of Materials Processing Technology 173, pp. 345–351, 2006
- Barton, K.L., Alleyne, A.G., *Cross-Coupled ILC for Improved Precision Motion Control: Design and Implementation*, American Control Conference, New York, 2007
- Biriș, C., *Contribuții privind optimizarea constructivă și funcțională a sistemelor de debitare cu comanda numerică*, teză de doctorat, Universitatea “Lucian Blaga” din Sibiu, 2006
- Breaz, R.E., **Tîrnovean, S.**, Biriș, C., Bologa, O.C., *Improving the Dynamic Behavior and Working Accuracy of the CNC Laser Cutting Machines*, 12th International Conference on Control, Automation, Robotics and Vision, ICARCV 2012, 5-7 December, Guangzhou, China, 2012
- Caydas, U., Hascalik, A., *Use of the grey ratioal analysis to determine optimum laser cutting parameters with multi-performance characteristics*, Optics & Laser Technology 40, pp. 987–994, 2008
- Cheng, T. et. al., *Intelligent Machine Tools in a Distributed Network Manufacturing Mode Environment*, International Journal of Advanced Manufacturing Technology, 17, pp. 221-231, 2001
- Chen J.M., Bao Y., Zuo T. Ch., *Laser CAM system for 3-dimensional laser cutting*, Journal of Materials Science Letters vol. 22, pp. 1791 – 1792, 2003
- Cheng, J.G., Zhang, J., Chu, C.C., Zhe, J., *Experimental Study and Computer Simulation of Fracture Toughness of Sheet Metal after Laser Forming*, The International Journal of Advanced Manufacturing Technology, vol. 26, nr. 11-12, pp. 1222-1230, 2005
- Cheng, M.Y., Lee, C.C., *Motion controller design for contour following tasks based on real-time contour error estimation*, IEEE Trans. Ind. Electron. 54(3), pp.1686–1695, 2007
- Chen, M., Ho, Y., Hsiao, W., Wu, T., Tseng, S., Huang, K., *Optimized laser cutting on light guide plates using grey ratioal analysis*, Optics and Lasers in Engineering, 49, pp. 222–228, 2011
- Choudhury, I., Shirley, S., *Laser cutting of polymeric materials: An experimental investigation*, Optics & Laser Technology, 42, pp. 503–508, 2010
- Davim, P., Barricas, N., Conceicao, M., Oliveira C., *Some experimental studies on CO2 laser cutting quality of polymeric materials*, Journal of Materials Processing Technology 198, pp. 99–104, 2008
- Dubey, A., Yadava, V., *Laser beam machining - A review*, Int. Journal of Machine Tools & Manufacture 48, pp. 609–628, 2008
- Eltawahni, H., Olabi, A., Benyounis, K., *Investigating the CO2 laser cutting parameters of MDF wood composite material*, Optics & Laser Technology 43, pp. 648–659, 2011
- Erkorkmaz, K., Altintas, Y., *High-speed CNC system design, part III: high-speed tracking and contouring control of feed modes*, Int. J. Mach. Tools. Manuf. 41, pp. 1637–1658, 2001

- Hewett, J., *Laser water jet cools and cuts in the material world*, Optics & Laser Europe no.3, martie 2007
- Huehnlein, K., Tschirpke, K., Hellmann, R., *Optimization of laser cutting processes using design of experiments*, Physics Procedia 5, pp. 243–252, 2010
- Immonen, E., Pohjolainen, S., *Feedback and Feedforward Output Regulation of Bounded Uniformly Continuous Signals for Infinite-Dimensional Systems*, SIAM Journal on Control and Optimization, vol. 45, nr. 5 (nov. 2006), pp. 1714 – 1735, 2006
- Isarie, I., *Tehnologia materialelor: Curs pentru uzul studenților, Vol. 1*, Institutul de Învățământ Superior Sibiu, 1980
- Isarie, C., *Contribuții privind prelucrarea materialelor compozite prin eroziune electrică cu electrod filiform*, teză de doctorat, Universitatea “Lucian Blaga” din Sibiu, 2006
- Kurt, M., Kaynak, Y., Bagci, E., Demirer, H., Kurt, M., *Dimensional analyses and surface quality of the laser cutting process for engineering plastics*, International Journal of Advanced Manufacturing Technology 41, pp. 259–267, 2009
- Kuznetsov, S.I., Shubladze, A.M., *On the possibility of PID control of the standard inertial and oscillatory plants*, Automation and Remote Control, vol. 68, nr. 7 (iul. 2007), pp. 1134 – 1144, 2007
- Lei, W.-T., Hsu, Y.-Y., *Accuracy enhancement of five-axis CNC machines through real-time error compensation*, International Journal of Machine Tools & Manufacture 43, pp. 871–877, 2003
- Mei, X., Tsutsumi, M., Tao, T., Sun, N., *Study on the compensation of error by stick-slip for high-precision table*, International Journal of Machine Tools & Manufacture 44, pp. 503-510, 2004
- Meijer J., *Laser beam machining (LBM), state of the art and new opportunities*, J. Mater. Process. Technol. 149, pp. 2–17, 2004
- Nemeș, T., Petrescu, V., *Tehnologia materialelor, vol.2: Elaborarea și procesarea materialelor metalice*. Editura Universității "Lucian Blaga" din Sibiu, Sibiu, 2001
- Oberg, E. ș.a., *Machinery's Handbook, 27th Ed.*, Industrial Press Inc., New York, 2004
- Pallett, R.J., Lark, R.J., *The use of tailored blanks in the manufacture of construction components*, J. Mater. Process. Technol. 117, pp. 249–254, 2001
- Park, H., *Optimal single biarc fitting and its applications*, Computer-Aided Design and Applications 1(1–4) pp. 187–195, 2004
- Park, H., Ahn, D.-G., *Knowledge-based CNC torch path generation for laser cutting of planar shapes*, International Journal of Advanced Manufacturing Technology, 37, pp. 302-313, 2008
- Petrescu, V., Nemeș, T., *Tehnologia materialelor, vol.1: Elaborarea și procesarea materialelor metalice*. Editura Universității "Lucian Blaga" din Sibiu, Sibiu, 2001
- Powell, P.J., *Solid State Lasers Stand Their Manufacturing Ground*, Photonics Spectra, oct. 2003, pp. 92-93, 2003
- Quintero, F., Varas, F., Pou, J., Lusquinos, F., Boutinguiza, M., Soto, R., Perez-Amor, M., *Theoretical analysis of material removal mechanisms in pulsed laser fusion cutting of ceramics*, J. Phys. D: Appl. Phys. 38, pp. 655–666, 2005
- Riveiro A., Quintero F., Lusquinos F., Comesana R., Pou J., *Parametric investigation of CO2 laser cutting of 2024-T3 alloy*, J. Mater. Process. Technol. 210, pp. 1138–1152, 2010

Shin, Y.T., Chen, C.S. Lee, A.C., *A novel cross-coupling control design for Bi-axis motion*, Int. J. Mach. Tools. Manuf. 42(14), pp. 1539–1548, 2002

Smith, C.A., *Automated Continuous Process Control*, John Wiley and Sons, Inc., New York, 2002

Stournaras A., Stavropoulos P., Salonitis K., Chryssolouris G., *An investigation of quality in CO2 laser cutting of aluminum*, CIRP J. Manuf. Sci. Technol. 2, pp. 61–69, 2009

Sundar, J.K.S., Thawari, G., Sundararajan, G., Joshi, S.V., *Influence of process parameters during pulsed Nd:YAG laser cutting of nickel-base superalloys*, J. Mater. Process. Technol. 170, pp. 229–239, 2005

Tera, M, Bologna, O., Breaz R., **Tîrnovean, S.**, *Study of Incremental Deep-Drawing of Bimetallic Sheets*, 2012 International Conference of Manufacturing Systems, ICMAS 2012, 8-9 November, București, România, 2012

Tîrnovean, S., et al, *Simulation Tools for Studying the Behavior of CNC Laser Cutting Machines in Different Working Modes*, 16th International Conference on System Theory, Control and Computing, 12-14 October, Sinaia, România, 2012

Vida-Simiti, I., ș.a., *Prelucrabilitatea materialelor metalice*, Editura Dacia, Cluj-Napoca, 1996

Wang, S.M., Liu, Y.L., Kang, Y., *An efficient error compensation system for CNC multi-axis machines*, International Journal of Machine Tools & Manufacture 42, pp. 1235–1245, 2002

Wang, S.-M., Yu, H.-J., Liao, H.-W., *A new high-efficiency error compensation system for CNC multi-axis machine tools*, International Journal of Advanced Manufacturing Technologies 16, published on-line, 2005

Wee, L.M., Li, L., *An analytical model for striation formation in laser cutting*, Appl. Surf. Sci. 247, pp. 277–284, 2005

Yau, H.-T., Ting, J.-Y., Chuang, C.-M., *NC Simulation with dynamic errors due to high-speed motion*, International Journal of Advanced Manufacturing Technologies 23, pp. 577–585, 2004

Yilbas, B.S., *Laser cutting quality assessment and thermal efficiency analysis*, J. Mater. Process. Technol. 155–156, pp. 2106–2115, 2004

Yilbas, B.S., *Laser cutting of thick sheet metals: Effects of cutting parameters on kerf size variations*, J. Mater. Process. Technol. 201, pp. 285–290, 2008

Zhao, G., Zhang, Q., Jiang, J., *Study on Biaxial Linkage for Full-Closed AC Servo System with Modeling and Experiment*, Advanced Science Letters, Volume 4, Numbers 6-7, pp. 2009–2014(6), 2011

*** *Asociația Română pentru Tehnologii Neconvenționale*, <http://www.artn.ro>

*** *Industrial Laser Processes – An Introduction*. The Association For Manufacturing Technology, 1998

*** *Lasers, Optics & Photonics Resources and News*, IOP Publishing, <http://www.optics.org>

**** *The Fascinating World of Sheet Metal*, Publisher and Editor, Trumpf GmbH + Co, KG, Ditzingen, Dr. Josef Raabe Verlags GmbH, 1996

*** *User's Guide. The Student Edition of MATLAB: The Ultimate Computing Environment for Technical Education*, Mathworks, Inc., Prentice Hall, Upper Saddle River, NJ, SUA, 1995